รายงานวิจัยฉบับสมบูรณ์

โครงการ การประยุกต์เทคนิคพาร์ทิเคิลสวอร์มสำหรับระบบผลิตไฟฟ้าด้วยพลังงานทดแทนภายใต้โครงการรับซื้อไฟฟ้าจากแหล่งผลิตไฟฟ้าขนาดเล็กมาก

Application of Particle Swarm Technique for Renewable Energy Power Systems under VSPP Project

โดย ผู้ช่วยศาสตราจารย์ ดร.นภาพร พ่วงพรพิทักษ์

มิถุนายน 2555

สัญญาเลขที่ MRG 5380276

รายงานวิจัยฉบับสมบูรณ์

โครงการ การประยุกต์เทคนิคพาร์ทิเคิลสวอร์มสำหรับระบบผลิตไฟฟ้าด้วยพลังงานทดแทน ภายใต้โครงการรับซื้อไฟฟ้าจากแหล่งผลิตไฟฟ้าขนาดเล็กมาก

Application of Particle Swarm Technique for Renewable Energy Power Systems under VSPP Project

ผู้ช่วยศาสตราจารย์ ดร.นภาพร พ่วงพรพิทักษ์
คณะวิทยาศาสตร์และวิศวกรรมศาสตร์
มหาวิทยาลัยเกษตรศาสตร์ วิทยาเขตเฉลิมพระเกียรติ จังหวัดสกลนคร

สนับสนุนโดยสำนักงานคณะกรรมการการอุดมศึกษา สำนักงานกองทุนสนับสนุนการวิจัย และ มหาวิทยาลัยเกษตรศาสตร์

Application of Particle Swarm Technique for Renewable Energy Power Systems under VSPP Project

Assistant Professor Dr.Napaporn Phuangpornpitak

A Research Submitted to the Office of the Higher Education Commission,
the Thailand Research Fund and Kasetsart University for the New Researchers Grant

June 2012

Acknowledgments

The author wishes to express her heart-felt gratitude and sincere appreciation to Associate Professor Dr.Suvit Tia, her mentor, for his valuable guidance, constructive suggestions, and incessant encouragement throughout this research work. She is thankful to his interest in the progress of her research plan that made this research a success.

She would like to express her sincere thanks and gratitude to the Office of the Higher Education Commission, the Thailand Research Fund (TRF) and the Kasetsart University Research and Development Institute (KURDI) for awarding her the New Researchers Grant. She also conveys her sincere thanks to the Center of Advanced Studies in Industrial Technology, Faculty of Engineering, Kasetsart University.

Thanks are due to Department of Electrical and Computer Engineering, Faculty of Science and Engineering, Kasetsart University, Chalermphrakiat Sakonnakhon Province Campus, and the Research and Development Institute of Chalermphrakiat Sakonnakhon Province Campus for their support during her research period.

There are special persons to whom this work is dedicated: her beloved family-parents, her brother and her friends. They have been an inexhaustible source of encouragement and moral support. Their understanding helped her in numerous ways to achieve her academic goal.

Abstract

PV distributed generation systems can make a positive contribution to the sustainability in developing countries that have access to electricity grid. Thailand is a tropical country and has plenty of sunshine. Therefore, the country has abundant of solar resource to generate electricity. Integration of solar photovoltaic system with grid connection would assist in supplementing the continually increasing of electricity need in Thailand. Greater use of PV distributed generation systems can also increase reliability of the electricity grid. Many problems exist arising from the operation of PV distributed generators jointly with the grid. Particularly, optimal placement and sizing of such system need to be optimized for improving voltage support in distribution networks. Therefore, it is necessary to take into account optimal allocation and sizing of PV grid connected in distribution systems during the design stage.

With the increase of PV distributed generation systems that are happening nowadays, the application of particle swarm technique which is the useful tool for system design and sizing for an actual feeder are presented in this study. The methodology applies the Particle Swarm Optimization (PSO) in order to minimize the system loss. Minimum system losses are obtained subjected to power constraint, voltage constraint and current limit. The methodology is tested on the 26-bus and the 59-bus radial distribution systems modified from the PEA distribution systems. The results indicate that the optimal placement and sizing of DG could be found using the application of PSO. The optimal DG can reduce the system losses.

Keywords: *Distributed Generation (DG), Particle Swarm Optimization (PSO), Photovoltaic (PV), PV distributed generation system, Very Small Scale Power Producer (VSPP)*

Table of Contents

List of Figures

List of Tables

Table **Description** **Page**

List of Abbreviations

The abbreviations used in the report are listed below. Any minor departure from this abbreviation is explained in the text itself.

Abbreviation	Description
C_1, C_2	Weighting factor
C_g	Acceleration constant of the best global value
$C_{g,f}$	Final value of social acceleration coefficient
$C_{g,i}$	Initial value of social acceleration coefficient
C_p	Acceleration constant of the best personal value
$C_{p,f}$	Final value of cognitive acceleration coefficient
$C_{p,i}$	Initial value of cognitive acceleration coefficient
C_l	Acceleration constant of the best local value
C_n	Acceleration constant of the best near neighbor value
g_d^k	Global best particle for dimension *d* at iteration *k*
$g_{i,pop}^k$	Probability value of the global best particle at iteration *k*
gen	Maximum number of generations to run
G_{best}	Global best of the group
k	Iteration
$k_{\max}$	Maximum iteration limit
$l_{i,d}^k$	Best position found in local particles group
$Loss_k$	Distribution loss at section *k*
n	Constant to set partition of sigmoid function
$n_{i,d}^k$	Near neighbor best
N_{SC}	Total number of sections
$p_{i,d}^k$	Best position of particle *i* for dimension *d* at iteration *k*
$p_{i,pop}^k$	Probability value of the best position of particle *i* at iteration *k*
P_{best_i}	Personal best of particle *i*
$P_{D,i}$	Real power demand at bus *i* (MW)
$P_{PV,i}$	Real power generation of PV at bus *i* (MW)
P_i	Net real power injection in bus *i* (MW)
P_{loss}	Power loss in the system (MW)

Abbreviation	**Description**
Q_i	Net reactive power injection in bus *i* (MVAR)
R	Chosen number between 1 and 10
R_1, R_2, R_3, R_4, R_5	Random numbers between 0 and 1
R_{ij}	Line resistance between bus *i* and *j* (ohm)
u	Constant to adjacent sharpness of the function
$v_{d,\max}$	Maximum velocity limit for dimension *d*
v_i^k	Current velocity of particle *i* at iteration *k*
v_i^{k+1}	Modified velocity of particle *i*
$v_{i,d}^k$	Velocity of particle *i* for dimension *d* at iteration *k*
$v_{i,d}^{k+1}$	Updated velocity of particle *i* for dimension *d* at iteration *k*
$v_{i,pop}^k$	Probability current velocity of particle *i* at iteration *k*
$v_{i,pop}^{k+1}$	Probability modified velocity of particle *i*
V_i	Voltage at bus *i* (kV)
w	Weighting function
w_{end}	Inertia weight at the end
$w_{\max}$	Maximum inertia weight
$w_{\min}$	Minimum inertia weight
w_{start}	Inertia weight at the start
w^k	Inertia weight at iteration *k*
$x_{d,\max}$	Maximum position of particle on dimension *d*
$x_{d,\min}$	Minimum position of particle on dimension *d*
x_i^k	Current position of particle *i* at iteration *k*
x_i^{k+1}	Modified position of particle *i*
$x_{i,d}^k$	Position of particle *i* for dimension *d* at iteration *k*
$x_{i,d}^{k+1}$	Updated position of particle *i* for dimension *d* at iteration *k*
$x_{i,pop}^k$	Probability value of the current position of particle *i* at iteration *k*
$x_{i,pop}^{k+1}$	Probability value of the modified position of particle *i*
δ_i	Angle at bus *i* (rad)

Chapter 1

Introduction

1.1 Background and Rationale

Distributed Generation in a Changing World

Although rural populations without electricity are expected to gradually decline, 95% of population growth over the next 30 years destined to take place in urban areas [1,2]. Developing countries therefore have to invest in the extension of electricity grid in urban areas. At present, distributed generation (DG) is gaining progressive acceptance virtually in all countries of the world, especially in the developing countries of Asia [3]. DG is the electricity generation at the point of use, including on-site generation that is connected to the grid [4]. The businesses or entrepreneurs who produce on site power can sell their electricity back to the grid. The key advantages of DG are the reduction of CO_2 emission and the improvement of power supply reliability.

PV Distributed Generation

Among the application of renewable energy technologies (RETs) for distributed generation, solar photovoltaic (PV) energy is growing rapidly. Though costs of PV systems have reduced significantly in the past decade, the installation costs are still ten times greater than those of conventional systems [3]. PV is not yet financially attractive at present prices. However, technological improvement would make the price of imported PV components decrease which make PV system would be attractive. The installed capacity of grid connected PV systems have grown dramatically over the last five years [5]. Greater use of PV distributed generation systems can also increase reliability of the electricity grid. Recently the peak power in PV grid connected system has reached about MWp while the experience in operating PV distributed generation is limited [6]. Medina [7] has noted that many problems exist arising from the operation of PV distributed generators jointly with the grid. Particularly, optimal placement and sizing of such system need to be optimized for improving voltage support in distribution networks. Therefore, it is necessary to take into account optimal allocation and sizing of PV grid connected in distribution systems during the design stage.

Optimal Placement and System Sizing Using Particle Swarm Technique

Particle Swarm Optimization (PSO) is an optimization technique based on the movement and intelligence of swarms. AlRashidi and El-Hawary [8] have noted the advantages of PSO technique over other optimization techniques as it is easy to implement and program with basic mathematical and logic operations.

Phuangpornpitak et al. [9] has surveyed the application of PSO technique for renewable energy power systems during the last decade. The details of the research characteristics, methodology used, objective and results obtained have been presented. Summary of work done in PSO technique for renewable energy power systems can be classified according to the research characteristics as follows: giving the concept of PSO as well as pros and cons, proposing a new PSO, application of PSO technique for the problem of design and sizing, system reliability, generation scheduling and load demand forecasting, etc. To select appropriate location and to determine DG size with minimum power losses, PSO would be one of the attractive methods to be employed as a tool.

Many PV distributed generation systems have been installed in Thailand in recent years. With the increase of PV distributed generation systems that are happening nowadays, the application of PSO technique which is the useful tool for system design and sizing for an actual feeder are presented in this study.

Research Questions Considered for the Study

The electricity access in Thailand covers 99.9%, and the remaining 0.1% are located in rural areas which do not have access to the services by traditional methods [1]. Although rural populations without electricity are expected to gradually decline, 95% of population growth over the next 30 years destined to take place in urban areas [1,2]. Developing countries therefore have to invest in the extension of electricity grid in urban areas.

Recognizing the advantages of PV distributed generation for the large scale systems connected to grid electricity, many such systems have been installed worldwide and in Thailand in recent years. However, to achieve commercialization and widespread use, the issue related to the design and sizing of the system needs to be addressed. This would be useful to developers and practitioners of renewable energy systems and to policy makers.

Earlier experiences indicate that there are problems arising from the operation of PV distributed generators jointly with the grid, particularly optimal placement and sizing of such system [7,10]. Therefore, there is a need to study the optimum allocation and sizing of PV distributed generation system. The following questions are addressed in this research:

- What are the optimum allocation issues and sizing aspects for adding PV to a distribution network to meet the load of the selected area?

- How to development of a suitable and effective model that includes optimum allocation issues and sizing aspects of PV distributed generation system to supply electricity in the selected area? This would assist policy makers, developers and installers of PV distributed generation systems to provide a reliable PV system based electricity supply.

1.2 Objective, Scope and Limitation

The overall objective of this research is to address the issues related to the optimum allocation and system sizing of PV distributed generation system. The specific objectives are as follows:

- To develop the PSO model with the optimal PV distributed generation placement. This would be useful to determine the optimal allocation and sizing of PV grid connected in distribution systems during the design stage.

- To find the optimal size and location of PV distributed generation system to minimize power loss.

The develop models are tested on a radial distribution system which is applied with PV distributed generation system. The power balance constraint is considered in the study.

1.3 Organization of Research Report

The entire research report is organized as follows:

Chapter 2 presents a survey of literature covering aspects related to the optimum allocation and sizing of the PV distributed generation system. The literature also covers the review of particle swarm technique for renewable energy power systems and further details on the research gaps that have been identified.

Chapter 3 discusses the methodology used in the study.

The fourth chapter provides details regarding the modeling of distributed generation system. This model was developed by considering optimum allocation issues and sizing aspects.

In Chapter 5, the details of experimentation carried out on the distributed generation systems are discussed. The applicability of PSO for optimal placement and sizing of the distributed generation system is discussed considering the case of PEA distribution networks. The results obtained by the application of the model are also presented.

Chapter 6 gives the contribution of the study. The proposed method for solving optimal number and size of PV unit placement on a radius system are discussed.

Finally, Chapter 7 presents the conclusions of this study and recommendations made for further research on the subject.

Chapter 2

Literature Review

Recently, PSO has been successfully applied to the various fields of power system including economic dispatch problems. This chapter presents the survey of PSO in solving optimization problems in electric power systems. The overview section provides the new way to implement renewable energy power system using particle swarm technique. Subsequent sections cover recent trends of PSO development in renewable energy power systems. This technique would be useful to determine the powerful energy management strategy so as to meet the required load demand at minimum operating cost while satisfying system equality and inequality constraints.

2.1 Overview of Particle Swarm Technique for Renewable Energy Power Systems

Fossil-based energy resources utilization increases global warming leading to climate change. All planet entities are therefore affected as impacts are felt all over the world. As a solution for the high prices of conventional fossil fuel energy sources and serious environmental problems, focus on promotion of cleaner, more efficient and less polluting sources and technologies, along with greater use of indigenous forms of renewable energy has been increasing around the world.

The utilization of renewable energy resources is becoming financially feasible for electrification due to the rapid development of the new technologies [11-13]. Power may be generated from a variety of sources using biomass, wind, solar, hydro-generators or hybrid combinations of these. Many studies show that these technologies could provide reliable and comparatively low cost electricity service [14,15]. Of the available renewable energy technologies (RETs), solar photovoltaic (PV) energy seems to be the fastest growing technology as its cost is declining during the last decade with technological improvements and economies of scale in production. Application of PV system has great potentials to meet the energy needs in a cost effective way by using a smart energy management strategy.

This chapter aims to address the PSO technique for the renewable energy power systems[*] [9]. PSO technique would be a useful tool to determine the powerful energy management strategy so as to meet the required load demand at minimum operating cost while satisfying system equality and inequality constraints.

---

[*] Part of this study has been published as a conference paper in the *PEA-AIT International Conference on Energy and Sustainable Development: Issues and Strategies (ESD 2010)* (N. Phuangpornpitak et al., 2010)

2.2 Concept of PSO Technique

PSO is an optimization technique based on the movement and intelligence of swarms. PSO applies the concept of social interaction to problem solving. It was developed in 1995 by James Kennedy (social-psychologist) and Russell Eberhart (electrical engineer) [16]. Particle swarm is the system model or social structure of basic creature which make a group to have some purpose such as food searching. It is an important part to take the most of population in a group that has the same activity. The group of creatures has this relative behavior, for example, bee swarm, fish school and bird flock.

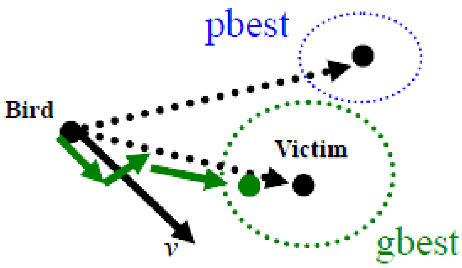

Figure 2.1: Birds' food searching with PSO
[17]

Fig. 2.1 shows bird flock hunter that is a bird suspect to a particle [17]. In victim searching, all bird groups will fly together in the same direction and the bird leader is the nearest food that has the shortest distance as the best fitness and the other birds follow the leader. The particle swarm model will be used by fitness value consideration. The particles represent solutions of fitness value. Moreover the important property in food searching of birds for instance, the particle's velocity of each particle uses to set the direction of particle movement. After that, all particles in the flock would be improved their directions that related with the best fitness of particle direction. The result of this process thus helps to set the most appropriate direction.

PSO consists of a group (swarm) of individuals (particles) moving in the search space looking for the best solution. Each particle is represented by a vector s of length n indicating the position and has a velocity vector v used to update the current position which adjusts its flying according to its own flying experience as well as the flying experience of other particles. Each particle keeps track of its coordinates in the solution space which are associated with the best solution (fitness) that has achieved so far by that particle. This value is called personal best, *Pbest*. Another best value that is tracked by the PSO is the best value obtained so far by any particle in the neighborhood of that particle. This value is called *Gbest*.

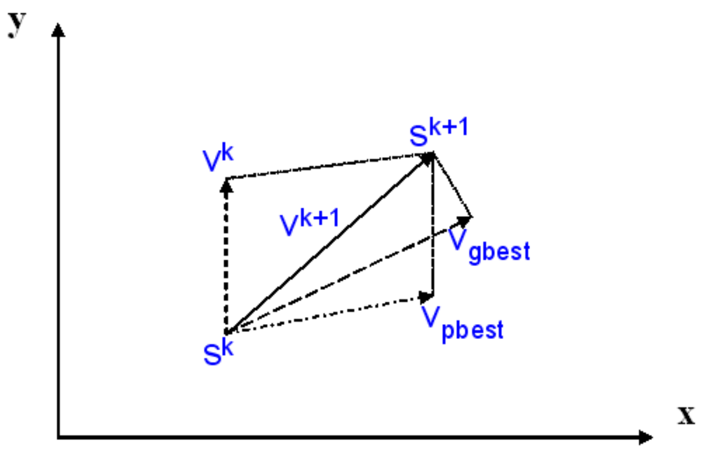

Figure 2.2: Concept of modification of a searching point by PSO
[17]

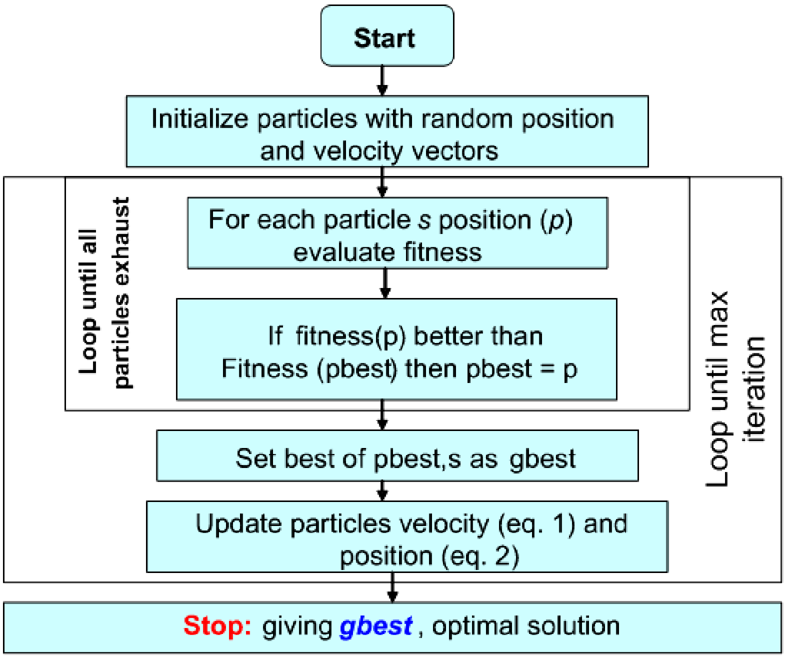

Figure 2.3: Flowchart of PSO algorithm
[18]

The basic concept of PSO lies in accelerating each particle toward its *Pbest* and the *Gbest* locations, with a random weighted acceleration at each time step as shown in Fig. 2.2. Each particle tries to modify its position using the following information with the flowchart of PSO algorithm as depicted in Fig. 2.3.

- the current positions,
- the current velocities,
- the distance between the current position and *Pbest*,
- the distance between the current position and *Gbest*.

The modification of the particle’s position can be mathematically modeled by using equations (2.1) and (2.2) [17]:

$$v_i^{k+1} = wv_i^k + C_1R_1(P_{best_i} - x_i^k) + C_2R_2(G_{best} - x_i^k) \tag{2.1}$$

$$x_i^{k+1} = x_i^k + v_i^{k+1} \tag{2.2}$$

where

C_1, C_2	:	Weighting factor,
R_1, R_2	:	Random numbers between 0 and 1,
w	:	Weighting function,
v_i^k	:	Current velocity of particle *i* at iteration *k*,
v_i^{k+1}	:	Modified velocity of particle *i*,
x_i^k	:	Current position of particle *i* at iteration *k*,
x_i^{k+1}	:	Modified position of particle *i*,
P_{best_i}	:	Personal best of particle *i*,
G_{best}	:	Global best of the group.

AlRashidi M.R. and El- Hawary M.E. [8] have noted the advantages of PSO technique over other optimization techniques as follows:

- It is easy to implement and program with basic mathematical and logic operations,
- It can handle objective functions with stochastic nature, like in the case of representing one of optimization variables as random, and
- It does not require the good initial solution to start its iteration process.

However, the drawbacks of PSO technique still exist as follows [8]:

- More parameters tuning is required, and
- Programming skills are required to develop and modify the competing algorithm to suit different optimization problems.

2.3 Application of PSO Technique for Renewable Energy Power Systems

A survey of PSO technique for renewable energy power systems during the last decade is presented in Table 2.1. The table presents details of the research characteristics, methodology used, objective and results obtained. Summary of work done in PSO technique for renewable energy power systems can be classified according to the research characteristics as follows: giving the concept of PSO as well as pros and cons, proposing a new PSO, application of PSO technique for the problem of design and sizing, system reliability, generation scheduling and load demand forecasting, etc.

Table 2.1: Summary of work done in PSO technique for renewable power systems

Research characteristics	**Methodology used**	**Objective/ Results obtained**	**Author name/ year**
* Present a concept as well as pros and cons of PSO in the area of electric power system	* Discuss PSO applications and its potential study in the future, for example, protection, restoration, its capability to improve accuracy and computation time, etc.	* Survey and summarize the PSO application in the area of electric power systems: • Economic dispatch, • Reactive power control and power losses reduction, • Optimal power flow, and power system controller design	Kennedy, J. and Eberhart, R., 1995 [16] AlRashidi, M.R. and El-Hawary, M.E., 2009 [8] El-Fouly, T.H.M., Zeineldin, H.H., El-Saadany, E.F. and Salama, M.M.A., 2008 [19]
* Propose an adaptive weight PSO for solving optimal distributed generation placement	* Apply adaptive PSO technique with the distributed generation placement	* Test results indicate that the PSO based algorithm is efficiently finding the optimal distributed generation placement	Prommee, W. and Ongsakul W., 2008 [17]
* Apply PSO technique for the problem of design and sizing in electric power systems	* Consider the system cost as the objective function, and use PSO algorithm for optimal sizing of the system's components	* Aim to minimize the total costs of the system such that satisfy the load demand	Hakimi, S.M. and Moghaddas-Tafreshi, S.M., 2009 [20], Kornelakis, A. and Marinakis, Y., 2009 [21 Gómez, M., López, A., and Jurado, F., 2010 [22] Kashefi Kaviani, A., Riahy, G.H., and Kouhsari, S.M., 2009 [23]

Table 2.1: Summary of work done in PSO technique for renewable power systems (Continued)

Research characteristics	**Methodology used**	**Objective/ Results obtained**	**Author name/ year**
* Apply PSO technique for the problem of system reliability	* Consider the reliability indices and use PSO algorithm for optimal sizing of the system's components * The reliability indices has been considered as follows: • Loss of load expectation, • Loss of energy expectation, • Loss of power supply probability	* Aim to improve the system reliability	Lingfeng, W. and Singh, C., 2009a [24] Lingfeng, W. and Singh, C., 2009b [25]
* Apply PSO technique for the problem of generation scheduling	* Consider the reserve requirement, load balance and RE resource availability constraints	* PSO technique can generate a near optimal schedule	Siahkali, H. and Vakilian, M., 2009 [26]
* Apply PSO technique for forecasting the energy demand	* Develop the energy demand scenario based on gross domestic product (GDP), population, import and export data	* The proposed model is proved to be a successful energy demand forecasting tool	Ünler, A., 2008 [27] El-Telbany, M. and El-Karmi, F., 2008 [28]

2.4 Conclusion

DG has the potential to be the planner's solution to various power system problems including system loss reduction. The appropriate size and location of DG is necessary as inappropriate placement may lead to even higher loss and hence increase the overall cost of the system operation. When DG is properly planned and operated they provide the benefit to the system in form of loss reduction in the network expansion. On the other hand, improper placement and operation will degrade the power quality, reliability and control of the power system.

The optimal placement and sizing of DG in distribution networks have been studied in order to achieve different targets. Earlier studies aim to minimize the system losses [29,30], minimize the network supply cost [31], and improve power quality [32]. The optimization techniques such as linear programming, dynamic programming, Genetic Algorithm and Particle Swarm Optimization have been employed to attain the aforementioned goals. The most striking difference between PSO and the other evolutionary algorithms is that PSO chooses the path of cooperation over competition. The other optimization algorithms commonly use some form of decimation, survival of the fittest. In contrast, the PSO population is stable and individuals are not destroyed or recreated. Individuals are influenced by the best performance of their neighbors. So, in PSO all the particles tend to converge to the best solution quickly, comparing with other evolutionary algorithms. In this study, PSO has been selected as a tool to find the appropriate location and size of DG on the distribution system.

The application of PSO in electric power systems would be useful for the utilities in developing countries which are facing the problem of high power loss in their distribution systems. This study would support the importance of selecting the correct size and suitable location for minimizing the power losses in the system.

Chapter 3

Methodology

The overall methodology adopted in carrying out the research is presented in this chapter.

3.1 Problem Formulation

The power loss reduction in a distribution system is required for efficient power system operation. The difference between the generated power and the demand will give the loss. The loss in the system can be calculated by equation (3.1) [33].

$$P_L = \sum_{i=1}^{n}\sum_{j=1}^{n} A_{ij}(P_iP_j + Q_iQ_j) + B_{ij}(Q_iP_j - P_iQ_j) \tag{3.1}$$

where

$$A_{ij} = \frac{R_{ij}\cos\left(\delta_i - \delta_j\right)}{V_iV_j}$$

$$B_{ij} = \frac{R_{ij}\sin\left(\delta_i - \delta_j\right)}{V_iV_j}$$

P_L	:	Power loss in the system (MW),
P_i	:	Net real power injection in bus *i* (MW),
Q_i	:	Net reactive power injection in bus *i* (MVar),
R_{ij}	:	Line resistance between bus *i* and *j* (ohm),
V_i	:	Voltage at bus *i* (kV),
V_j	:	Voltage at bus *j* (kV),
δ_i	:	Angle at bus *i* (rad),
δ_j	:	Angle at bus *j* (rad).

The proposed work aims at minimizing the objective function designed to reduce power loss. The main objective function is defined as equation (3.2) [33].

$$\text{Minimize} \quad P_L = \sum_{k=1}^{N_{SC}} Loss_k \tag{3.2}$$

Subject to the constraints as described in equations (3.3) to (3.5) [33].

Power balance constraints: $$\sum_{i=1}^{N} P_{DGi} = \sum_{i=1}^{N} P_{Di} + P_L \tag{3.3}$$

Voltage constraints: $$|V_i|^{\min} \le |V_i| \le |V_i|^{\max} \tag{3.4}$$

Current limits: $$|I_{ij}| \le |I_{ij}|^{\max} \tag{3.5}$$

where

$Loss_k$	:	Distribution loss at section *k*,
N_{SC}	:	Total number of sections,
P_{DGi}	:	Real power generation DG at bus *i* (MW),
P_{Di}	:	Real power demand at bus *i* (MW).

3.2 PSO Procedure

The flowchart of the proposed algorithm is illustrated in Fig. 3.1 [30]. The PSO-based approach for solving the optimal placement of distributed generation problem to minimize the loss takes the following steps:

Step 1: Input line and bus data, and bus voltage limits.

Step 2: Calculate the loss using distribution load flow based on backward-forward sweep.

Step 3: Randomly generates an initial population (array) of particles with random positions and velocities on dimensions in the solution space. Set the iteration counter $k = 0$.

Step 4: For each particle if the bus voltage is within the limits, calculate the total loss using equation (3.1). Otherwise, that particle is infeasible.

Step 5: For each particle, compare its objective value with *the individual best*. If the objective value is lower than *Pbest*, set this value as the current *Pbest*, and record the corresponding particle position.

Step 6: Choose the particle associated with the minimum *individual best Pbest* of all particles, and set the value of this *Pbest* as the current *overall best Gbest*.

Step 7: Update the velocity and position of particle using equations (2.1) and (2.2) respectively.

Step 8: If the iteration number reaches the maximum limit, go to Step 9. Otherwise, set iteration index $k = k + 1$, and go back to Step 4.

Step 9: Print out the optimal solution to the target problem. The best position includes the optimal locations and size of DG, and the corresponding fitness value representing the minimum power loss.

The PSO algorithm is able to reach a good solution by finite steps of evolution steps performed on a finite set of possible solutions. The objective function for the optimization is the power loss reduction as shown in equation (3.1). The PSO algorithm sets in the core of this optimization problem. This routine is programmed by MATLAB software.

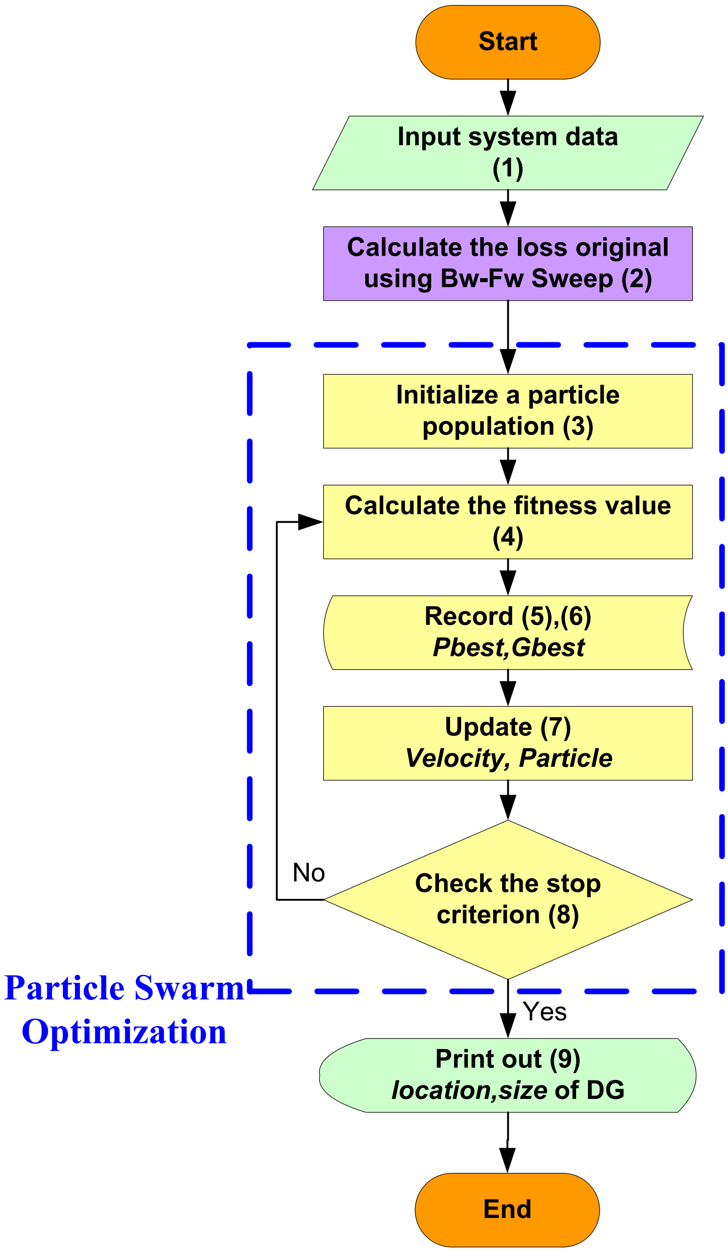

Figure 3.1: Flowchart of the implemented methodology [30]

3.3 Validation of the Proposed Model

The validation of the model has been carried out by considering a part of PEA distribution network. The model determines the optimal size and location of DG that should be placed in the system where maximum loss saving occurs. The proposed methods based on PSO algorithm can be favorable for solving distributed generation placement and its sizing.

An overview of the methodology of the study is given in this chapter. As described, the model of most favorable size and location of DG has been evaluated for its applicability and use by considering the real scale systems. Details of the model are discussed in Chapter 4. The procedures adopted, results obtained and the lessons learned from this study can be adopted to systems to be implemented in other distributed generation systems. Chapter 5 discusses the details of the study regarding the test system and analyses. Chapter 6 gives the contribution of this study. The proposed model for solving optimal number and size of PV unit problem on a radius system are discussed. Based on the work carried out in this study, the conclusions and the recommendations for further work are discussed in Chapter 7.

Chapter 4

PSO Modeling for Distributed Generation System

The details on PSO modeling of the optimum allocation issues and sizing aspects to the distributed generation system are described. The model equations used and the procedure adopted are presented. These models have been applied for the PEA distributed generation systems described in Chapter 5 and Chapter 6.

4.1 Overview of PSO Modeling

To know the applicability of PSO modeling for distributed generation system (in this study, the PV distributed generation system is considered), it is important to address the optimum allocation issues and sizing aspects of the purposed system [9]. Moreover, before the actual installation and implementation of hardware in the field, a systematic theoretical study needs to be carried out to assess whether the proposed approach of distributed generation system is suitable or not [34,35]. Therefore, modeling of any proposed system becomes necessary.

As discussed in Chapter 2, PSO is a population based search model including two main update equations: velocity and position updates. PSO modeling can be applied to solving the problem of renewable energy power systems, for example, design and sizing, system reliability, generation scheduling and load demand forecasting, etc.

For this study, various PSO models are used and compared in providing the optimal distributed generation placement. The following PSO models are discussed and analyzed:

- (i) Classical PSO (CPSO),
- (ii) PSO with time varying inertia weight (PSO-TVIW),
- (iii) Improved reinitialized social structure PSO (IRS-PSO),
- (iv) PSO with time varying acceleration coefficients (TVAC-PSO), and
- (v) Self-organizing hierarchical PSO with time varying acceleration coefficients (SHPSO-TVAC).

The improvements and the parameter used for different PSO models are discussed. The solution algorithm is also available for various PSO models since they adopt the same concept and update the method.

4.2 Classical PSO

Classical PSO (CPSO) is the original PSO model and it is the base model for many improved PSO versions. The classical PSO mathematical model proposed by James Kennedy (social-psychologist) and Russell Eberhart (electrical engineer) [16] consists of two main equations: velocity and position update equations which expressed as equations (4.1) and (4.2).

$$v_{i,d}^{k+1} = v_{i,d}^{k} + C_p R_1 (p_{i,d}^{k} - x_{i,d}^{k}) + C_g R_2 (g_d^{k} - x_{i,d}^{k}) \tag{4.1}$$

$$x_{i,d}^{k+1} = x_{i,d}^{k} + v_{i,d}^{k+1} \tag{4.2}$$

where

C_g	:	Acceleration constant of the best global value,
C_p	:	Acceleration constant of the best personal value,
R_1, R_2	:	Random numbers between 0 and 1,
$v_{i,d}^{k}$	:	Velocity of particle *i* for dimension *d* at iteration *k*,
$v_{i,d}^{k+1}$	:	Updated velocity of particle *i* for dimension *d* at iteration *k*,
$x_{i,d}^{k}$	:	Position of particle *i* for dimension *d* at iteration *k*,
$x_{i,d}^{k+1}$	:	Updated position of particle *i* for dimension *d* at iteration *k*,
$p_{i,d}^{k}$	:	Best position of particle *i* for dimension *d* at iteration *k*,
g_d^{k}	:	Global best particle for dimension *d* at iteration *k*.

4.3 PSO with Time Varying Inertia Weight

PSO with time varying inertia weight (PSO-TVIW) has been proposed by Shi and Eberhart [36,37], the method is updated to improve the location search precision by adding weight, the velocity is updated as equation (4.3) and the weight function is given as equation (4.4).

$$v_{i,d}^{k+1} = w^k v_{i,d}^{k} + C_p R_1 (p_{i,d}^{k} - x_{i,d}^{k}) + C_g R_2 (g_d^{k} - x_{i,d}^{k}) \tag{4.3}$$

$$w^k = w_{\max} - \left(\frac{w_{\max} - w_{\min}}{k_{\max}} \right) k \tag{4.4}$$

where

w^k	:	Inertia weight at iteration *k*,
$w_{\max}$	:	Maximum inertia weight,
$w_{\min}$	:	Minimum inertia weight,
k	:	Iteration,
$k_{\max}$	:	Maximum iteration limit.

The maximum and minimum weight values, $w_{\max}$ and $w_{\min}$ are set as 0.9 and 0.4, respectively. Particle positions are updated by equation (4.5).

$$x_{i,d}^{k+1} = x_{i,d}^{k} + v_{i,d}^{k+1} \tag{4.5}$$

4.4 Improved Reinitialized Social Structure PSO

Prommee and Ongsakul [38] proposed an improved reinitialized social structure particle swarm optimization (IRS-PSO) for solving optimal distributed generation placement in a minigrid system. The velocity and position update equations are given as equations (4.6) and (4.7).

$$v_{i,d}^{k+1} = w^k v_{i,d}^k + C_p R_1 (p_{i,d}^k - x_{i,d}^k) + C_g R_2 (g_d^k - x_{i,d}^k) + C_l R_3 (l_{i,d}^k - x_{i,d}^k) + C_n R_4 (n_{i,d}^k - x_{i,d}^k) \quad (4.6)$$

$$x_{i,d}^{k+1} = x_{i,d}^k + v_{i,d}^{k+1} \quad (4.7)$$

where

C_l	:	Acceleration constant of the best local value,
C_n	:	Acceleration constant of the best near neighbor value,
R_1, R_2, R_3, R_4	:	Random numbers between 0 and 1,
$l_{i,d}^k$	:	Best position found in local particles group,
$n_{i,d}^k$	:	Near neighbor best.

The IRS-PSO velocity includes an inertia term, a cognitive term and three social terms including g_d^k, $l_{i,d}^k$, and $n_{i,d}^k$. The weight formula of the IRS-PSO is shown as equation (4.8).

$$w^k = \frac{(w_{\max} - w_{\min})(k_{\max} - k)}{k_{\max} + w_{\min}} \quad (4.8)$$

4.5 PSO with Time Varying Acceleration Coefficients

PSO with time varying acceleration coefficients (TVAC-PSO) is an extensive version from PSO-TVIW proposed by Suganthan [39]. In the initial stages of the search of TVAC-PSO, particles are encouraged to roam individually through a wide search space. This is with a high acceleration factor of the cognitive component and a less acceleration factor of the social component in equation (4.3). The time varying acceleration coefficients of the cognitive and social components are determined by equations (4.9) and (4.10). Normally, the acceleration coefficients are in the range of 0.5 to 2.5 [39].

$$C_p = C_{p,i} - \left(\frac{C_{p,i} - C_{p,f}}{k_{\max}} \right) k \quad (4.9)$$

$$C_g = C_{g,i} - \left(\frac{C_{g,i} - C_{g,f}}{k_{\max}} \right) k \quad (4.10)$$

where

$C_{p,i}$	:	Initial value of cognitive acceleration coefficient,
$C_{p,f}$	:	Final value of cognitive acceleration coefficient,
$C_{g,i}$	:	Initial value of social acceleration coefficient,
$C_{g,f}$	:	Final value of social acceleration coefficient.

4.6 Self-Organizing Hierarchical PSO with Time Varying Acceleration Coefficients

Self-organizing hierarchical PSO with time varying acceleration coefficients (SHPSO-TVAC) is a novel PSO that preserves the effectiveness of TVAC-PSO for roaming towards the search space at the beginning. Boonchuay and Ongsakul [40] noted that the previous velocity term is made to zero to rush towards a local optimum solution. However, with this modification, particles lose the momentum to find better solutions in the later stage of the search. As the velocity update expression in equation (4.1), Ratnaweera et al. [41] propose the additional conditions of SHPSO-TVAC. Thus, SHPSO-TVAC can overcome this weakness by reinitialized the velocity vector of a particle whenever it stagnates during the search. Chaturvedi et al. [42] propose the maximum velocity limit for the dth dimension ($v_{d,\max}$) which calculated by equation (4.11).

$$v_{d,\max} = \frac{x_{d,\max} - x_{d,\min}}{R} \tag{4.11}$$

where

$v_{d,\max}$	:	Maximum velocity limit for the dth dimension,
$x_{d,\max}$	:	Maximum position of particle on the dth dimension,
$x_{d,\min}$	:	Minimum position of particle on the dth dimension,
R	:	Chosen number between 1 and 10.

The chosen value of R reflects the percentage of dynamic range of the solution on each dimension. Note that SHPSO-TVAC adopts the time-varying acceleration coefficients; equations (4.9) and (4.10) are still required.

4.7 Data Needed for the Model

In this study the PV grid connected system will be analyzed. Fig. 4.1 shows the block diagram of PV grid connection. On the main feeder (AC bus), multiple components of PV grid connection are jointed including PV array, DC/AC converter, AC bus and load. The power injection efficiency depends on solar radiation and weather conditions.

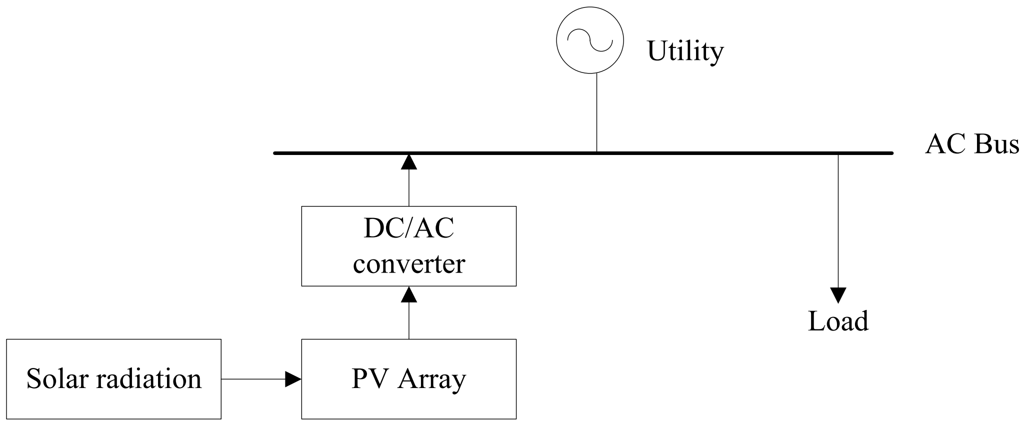

Figure 4.1: Block diagram of PV grid connection

The parameters used in the model are shown in Table 4.1, and most of these could be obtained from the substation of PEA, i.e. single line diagram, the bus characteristic and the line characteristic. This observes from a number of tests and applications in power system research areas. For a particular PSO application, optimal value of PSO parameters could be precisely provided based on empirical tests. These parameters are generally used. The input required and assumptions made with the procedure adopted are employed to obtain the minimum loss.

Table 4.1: Parameters used in the PSO model

Parameters	**Symbol**	**Unit**
Single line diagram		
Bus characteristic		
- Active load	P	MW
- Reactive load	Q	MVAR
Line characteristic		
- Line resistance	R	pu
- Line reactance	X	pu

Chapter 5

Results and Discussions

The details of experiments carried out on one part of the PEA distribution network are described in this chapter. The optimal DG placement using PSO modeling is tested on two different radial distribution systems. The two systems are the 26-bus radial system and the 59-bus radial system.

5.1 Optimal DG Placement of the 26-Bus Radial System

The microgrid distribution system (22 kV) is used as a test system. A system was selected from one part of the PEA central station distribution network. The single line diagram of the network is illustrated in Fig. 5.1. The 26-bus system has 25 sections with the total load of 8.49 MW and 5.28 MVAR. The original total real and reactive power losses of the system are 11.68 kW (0.14%) and 26.08 kVAR (0.49%), respectively. Tables 5.1 and 5.2 provide the data of buses and lines. The base MVA is 10 MVA and the base kV is 12.66 kV. Following analysis is performed with the test system and results are presented accordingly.

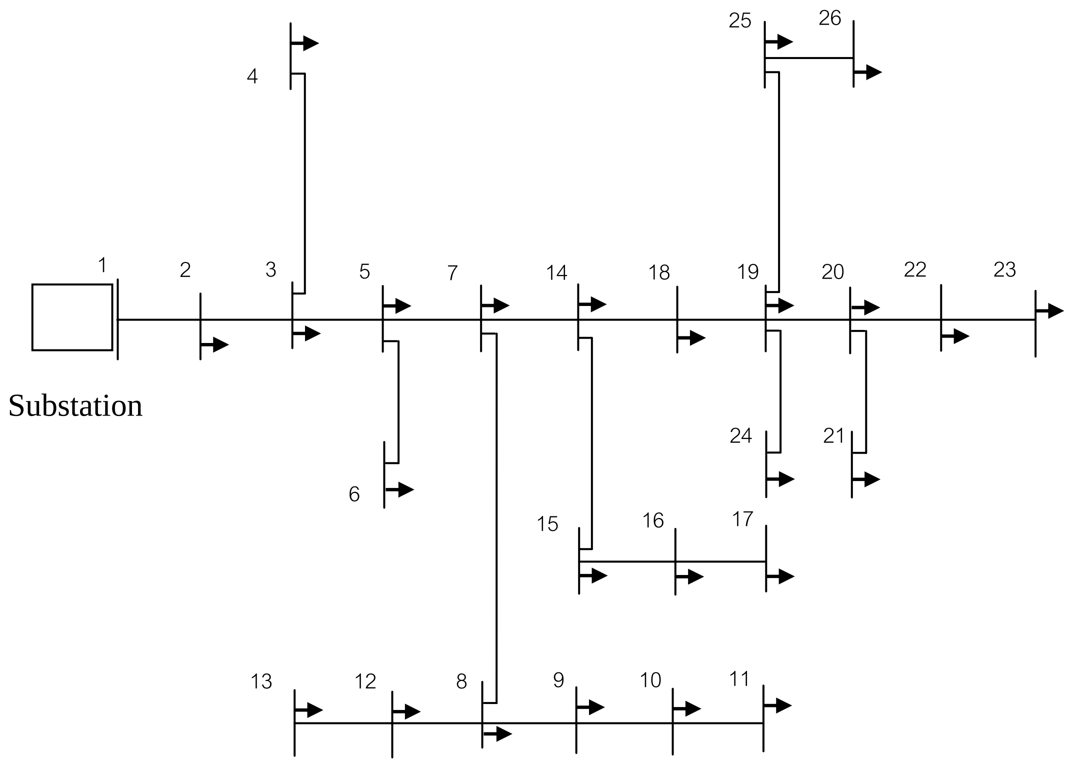

Figure 5.1: A 26-bus radial distribution system

Table 5.1: Bus characteristic of the 26-bus radial system

Bus characteristic		
Bus number	Load	
	P (MW)	Q (MVAR)
1	0.000	0.000
2	0.369	0.221
3	0.369	0.221
4	0.369	0.221
5	0.369	0.221
6	0.369	0.221
7	0.369	0.221
8	0.369	0.221
9	0.369	0.221
10	0.369	0.221
11	0.369	0.221
12	0.369	0.221
13	0.369	0.221
14	0.369	0.221
15	0.369	0.221
16	0.369	0.221
17	0.214	0.761
18	0.272	0.210
19	0.369	0.221
20	0.369	0.221
21	0.369	0.221
22	0.369	0.221
23	0.250	0.200
24	0.250	0.200
25	0.250	0.200
26	0.250	0.200

Table 5.2: Line characteristic of the 26-bus radial system

Line characteristic			
From	**To**	**R (pu)**	**X (pu)**
1	2	0.000177	0.000319
2	3	0.000469	0.001089
3	4	0.000054	0.000129
3	5	0.000362	0.000840
5	6	0.000053	0.000127
5	7	0.000067	0.000156
7	8	0.000253	0.000498
8	9	0.000068	0.000134
9	10	0.000192	0.000377
10	11	0.000040	0.000078
8	12	0.000301	0.000592
12	13	0.000127	0.000250
7	14	0.000336	0.000780
14	15	0.000022	0.000054
15	16	0.000032	0.000075
16	17	0.000015	0.000036
14	18	0.000415	0.000963
18	19	0.000090	0.000210
19	20	0.000881	0.002045
20	21	0.000204	0.000473
20	22	0.001626	0.003772
22	23	0.000014	0.000034
19	24	0.000128	0.000297
19	25	0.000845	0.001960
25	26	0.000919	0.002131

Fig. 5.2 shows the suitable DG size of a 26-bus test system and Fig. 5.3 shows the power loss of a 26-bus test system. The proposed methodology was run on a 26 bus test system. The impact of installing DG in the case study network with optimal allocation and sizing is presented Table 5.3. The decrease in total power loss depends on the location and size of DG. As shown in Table 5.3, the minimum power loss occurs in bus 14 (4.55 kW and 10.18 kVAR). The proposed method can reduce loss by 61% of its original loss.

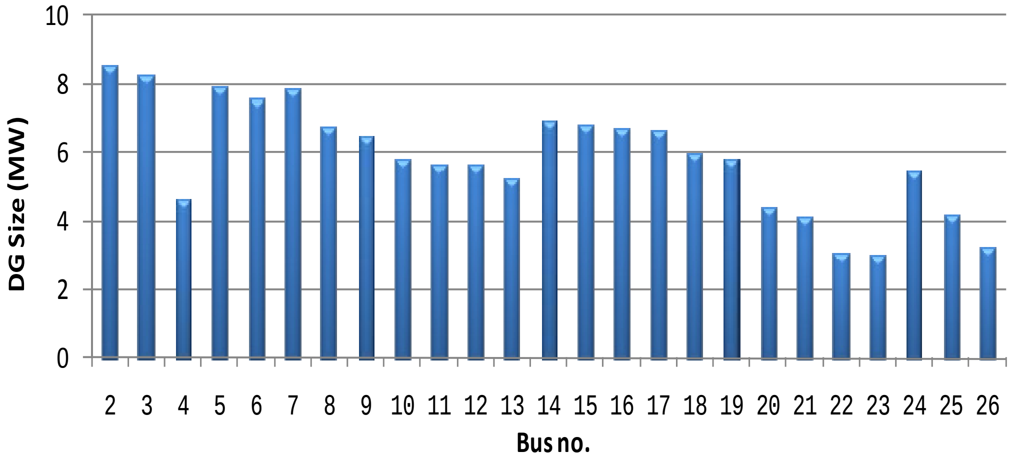

Figure 5.2: Suitable DG size of a 26-bus test system

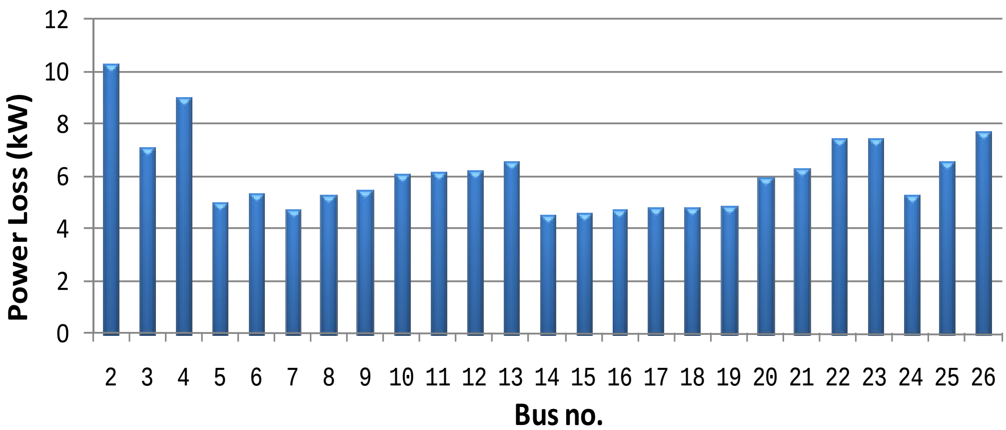

Figure 5.3: Power loss of a 26-bus test system

Table 5.3: Results of a 26-bus test system

Bus number	**DG size (MW)**	**P_{loss} (kW)**	**Q_{loss} (kVAR)**
2	8.5068	10.3303	23.6133
3	8.2344	7.0983	16.1083
4	4.6550	8.9869	18.2133
5	7.9302	5.0501	11.3533
6	7.5529	5.3496	12.0645
7	7.8503	4.7509	10.6558
8	6.7771	5.2995	11.7565
9	6.5012	5.5076	12.1832
10	5.8049	6.0814	13.3722
11	5.6715	6.2010	13.6210
12	5.6622	6.2157	13.6540
13	5.2797	6.5582	14.3781
14	***6.9498***	***4.5514***	***10.1737***
15	6.8578	4.6306	10.3651
16	6.7209	4.7580	10.6587
17	6.6550	4.8235	10.8134
18	5.9951	4.8151	10.7488
19	5.8298	4.8684	10.8650
20	4.4216	5.9569	13.3004
21	4.1464	6.2798	14.0268
22	3.0244	7.4421	16.6189
23	3.0156	7.4532	16.6450
24	5.4807	5.2573	11.7482
25	4.1998	6.5872	14.7431
26	3.2140	7.7049	17.2457

5.2 Optimal DG Placement of the 59-Bus Radial System

Another system was selected from one part of PEA distribution network. Fig. 5.4 shows the 59-bus system has 58 sections with the total load of 12.17 MW and 6.71 MVAR. The original total real and reactive power losses of the system are 122.49 kW (1.01%) and 279.41 kVAR (4.16%), respectively. For PSO parameters, the population size is 200 and the maximum generator (k_{max}) is 100.

Tables 5.4 and 5.5 provide the data of buses and lines. The analysis has been performed with the test system and results are presented in Table 5.6. The impact of installing DG in the case study network with optimal allocation and sizing are presented. The suitable bus for installing DG is bus 18, which indicated by the lowest power loss.

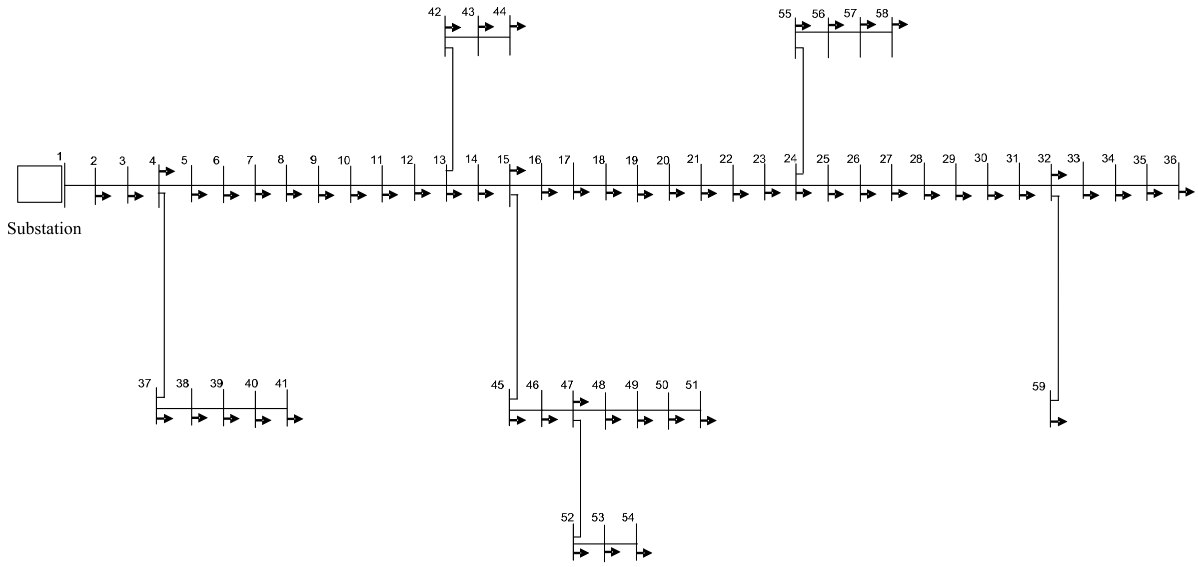

Figure 5.4: A 59 bus-radial distribution system

Table 5.4: Bus characteristic of the 59-bus radial system

Bus characteristic		
	Load	
Bus number	P (MW)	Q (MVAR)
1	0.000	0.000
2	0.276	0.152
3	0.018	0.010
4	0.088	0.048
5	0.551	0.305
6	0.276	0.152
7	0.276	0.152
8	0.088	0.048
9	0.350	0.194
10	0.276	0.152
11	0.551	0.305
12	0.018	0.010
13	0.350	0.194
14	0.044	0.024
15	0.551	0.305
16	0.044	0.024
17	0.276	0.152
18	0.276	0.152
19	0.018	0.010
20	0.350	0.194
21	0.044	0.024
22	0.018	0.010
23	0.276	0.152
24	0.044	0.024
25	0.350	0.194
26	0.044	0.024
27	0.276	0.152
28	0.044	0.024
29	0.018	0.010
30	0.276	0.152

Table 5.4: Bus characteristic of the 59-bus radial system (Continued)

Bus characteristic		
	Load	
Bus number	P (MW)	Q (MVAR)
31	0.044	0.024
32	0.350	0.194
33	0.551	0.305
34	0.088	0.048
35	0.276	0.152
36	0.276	0.152
37	0.088	0.048
38	0.088	0.048
39	0.088	0.048
40	0.276	0.152
41	0.088	0.048
42	0.088	0.048
43	0.044	0.024
44	0.350	0.194
45	0.276	0.152
46	0.551	0.305
47	0.276	0.152
48	0.551	0.305
49	0.018	0.010
50	0.088	0.048
51	0.276	0.152
52	0.018	0.010
53	0.044	0.024
54	0.350	0.194
55	0.276	0.152
56	0.350	0.194
57	0.044	0.024
58	0.276	0.152
59	0.018	0.010

Table 5.5: Line characteristic of the 59-bus radial system

Line characteristic			
From	**To**	**R (pu)**	**X (pu)**
1	2	0.000266	0.000617
2	3	0.000217	0.000504
3	4	0.000131	0.000304
4	5	0.001818	0.004217
5	6	0.000357	0.000852
6	7	0.000350	0.000811
7	8	0.000684	0.001587
8	9	0.000075	0.000174
9	10	0.000501	0.001161
10	11	0.000642	0.001488
11	12	0.000375	0.000870
12	13	0.001092	0.002533
13	14	0.000556	0.001290
14	15	0.000482	0.001117
15	16	0.000801	0.001858
16	17	0.000551	0.001084
17	18	0.000258	0.000507
18	19	0.000576	0.001134
19	20	0.000425	0.000835
20	21	0.000472	0.000928
21	22	0.000143	0.000282
22	23	0.000151	0.000296
23	24	0.000532	0.001047
24	25	0.000214	0.000421
25	26	0.000149	0.000294
26	27	0.000149	0.000294
27	28	0.001344	0.002644
28	29	0.000475	0.000935
29	30	0.000447	0.000880
30	31	0.002009	0.003952

Table 5.5: Line characteristic of the 59-bus radial system (Continued)

Line characteristic			
From	**To**	**R (pu)**	**X (pu)**
31	32	0.000755	0.001486
31	32	0.000755	0.001486
32	33	0.002040	0.004013
33	34	0.000679	0.001335
34	35	0.002319	0.004562
35	36	0.001262	0.002482
4	37	0.001210	0.000854
37	38	0.001210	0.000854
38	39	0.002456	0.001734
39	40	0.001239	0.000875
40	41	0.000146	0.000103
13	42	0.004377	0.002425
42	43	0.005415	0.003000
43	44	0.001897	0.001051
15	45	0.000436	0.001012
45	46	0.001850	0.004291
46	47	0.000437	0.001013
47	48	0.000822	0.001907
48	49	0.000505	0.001170
49	50	0.000932	0.002163
50	51	0.000453	0.000251
47	52	0.002631	0.001457
52	53	0.001095	0.000607
53	54	0.000306	0.000170
24	55	0.000205	0.000402
55	56	0.000424	0.000834
56	57	0.000356	0.000701
57	58	0.007182	0.005071
32	59	0.008451	0.005968

Table 5.6: Results of a 59-bus test system

Bus number	**DG size (MW)**	**P_{loss} (kW)**	**Q_{loss} (kVAR)**
2	12.3094	118.9338	271.1260
3	12.1804	115.6525	263.5049
4	12.1412	113.6753	258.9167
5	11.4653	89.3320	202.4503
6	11.3603	84.9935	192.0983
7	11.2485	80.9611	182.7540
8	11.0368	73.4914	165.4220
9	11.0162	72.6848	163.5507
10	10.8559	67.6922	151.9804
11	10.6599	61.6608	138.0005
12	10.5281	58.5868	130.8687
13	10.2247	49.5687	109.9502
14	10.0400	45.9386	101.5282
15	9.8985	42.7978	94.2496
16	9.4139	42.5514	93.6804
17	9.1281	42.2382	93.0746
18	**8.9983**	**42.1843**	**92.9904**
19	8.7171	42.2617	93.2263
20	8.5291	42.2389	93.2640
21	8.3225	42.4358	93.7685
22	8.2629	42.4890	93.9122
23	8.2014	42.5416	94.0575
24	7.9848	42.9207	94.9723
25	7.8853	43.4130	96.0306
26	7.8138	43.8320	96.9261
27	7.7436	44.2495	97.8207
28	7.1532	48.0977	106.1112
29	6.9706	49.2830	108.7118
30	6.8092	50.3262	111.0191

Table 5.6: Results of a 59-bus test system (Continued)

Bus number	**DG size (MW)**	**P_{loss} (kW)**	**Q_{loss} (kVAR)**
31	6.1598	54.9438	121.2940
32	5.9545	56.4171	124.6333
33	5.4442	60.6750	134.2404
34	5.2776	62.3029	137.8701
35	4.7811	67.3692	149.2592
36	4.5358	70.0241	155.2289
37	4.4305	119.1724	268.6182
38	2.9257	120.4224	272.4827
39	1.7896	121.1902	275.1623
40	1.5523	121.4419	276.0219
41	1.4957	121.4342	275.9991
42	6.3650	77.0117	145.8746
43	4.3394	89.9321	175.4291
44	3.9602	93.2707	184.7491
45	9.4964	45.1622	99.7400
46	8.1133	52.7801	117.4208
47	7.8387	54.6850	121.8409
48	7.3249	58.4328	130.5431
49	7.0241	61.0598	136.6355
50	6.5270	65.0996	146.0210
51	6.3102	67.0460	147.3873
52	6.3219	67.0691	133.0330
53	5.8592	71.0001	138.6170
54	5.7400	71.8918	139.8614
55	7.8863	44.4368	98.2229
56	7.6086	46.2979	102.0016
57	7.4237	48.7279	107.1960
58	4.7924	73.6337	141.4286
59	4.0056	78.8196	156.1706

5.3 Numerical Results

This section presents the numerical solution of the proposed methods: CPSO, PSO-TVIW, IRS-PSO, TVAC-PSO and SHPSO-TVAC for solving optimal DG placement in a microgrid system. The objective is to minimize the real power loss within power generation limits and voltage limits. The PVDG is considered in this study. The DG supplies real power only. Classical PSO (CPSO) is the traditional basic particle swarm technique. In PSO-TVIW approach, the inertia weight is decreasing during the solution search. The improved RS-PSO is improved by adding particle random to escape the local optimum and search for a new optimum solution in the process of velocity updating when particle values are out of limit. The movement of each particle in IRS-PSO is pulled by an inertia term, a cognitive term (personal best) and three social learning terms including global best, local best and near neighbor best. In PSO-TVAC approach, the acceleration coefficients are varied. A novel PSO version named SHPSO-TVAC approach includes the reinitializing process to improve searching performance.

Tables 5.7 – 5.12 show optimal DG location and sizes minimizing real power loss in the 26-bus and the 59-bus distribution systems. Single DG is considered in this study. The decrease in total real power loss will depend on the location and size of DG.

Table 5.7: Optimal single DG placement by five PSO types (Population = 200)

Method	**Bus No.**	**DG size (MW)**	**Real power loss (kW)**	**Reactive power loss (kVAR)**	**Time (second)**
The total original loss in the 26 bus PEA			11.6925	26.0812	
GA [43]	14	6.9510	4.5500	10.1900	n/a*
CPSO	14	6.4420	3.3386	10.2585	37.3600
PSO-TVIW	14	6.4468	***3.3386***	10.2571	35.6100
IRS-PSO	14	6.4470	3.3386	10.2570	***35.4060***
TVAC-PSO	14	6.4468	3.3386	10.2571	35.7970
SHPSO-TVAC	14	6.3810	3.3391	10.2786	35.6400
The total original loss in the 59 bus PEA			122.5559	278.8729	
GA [43]	18	9.0240	41.6200	91.7800	n/a
CPSO	18	9.0267	41.5706	91.6746	79.2810
PSO-TVIW	18	9.0119	***41.5704***	91.6779	***79.1400***
IRS-PSO	18	9.0080	41.5704	91.6789	79.9380
TVAC-PSO	18	9.0114	41.5704	91.6780	81.0320
SHPSO-TVAC	18	9.0129	41.5704	91.6776	80.3900

* n/a = not available

Fig. 5.5 shows the voltage level comparison for the 26-bus system with and without installation of PV system. Fig. 5.6 shows the voltage level comparison for the 59-bus system with and without installation of PV system.

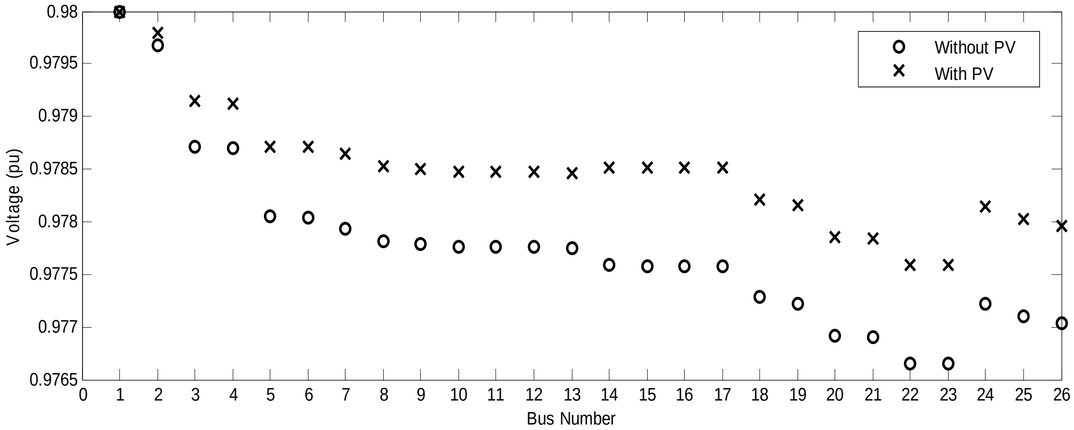

Figure 5.5: Voltage level comparison on the 26-bus system

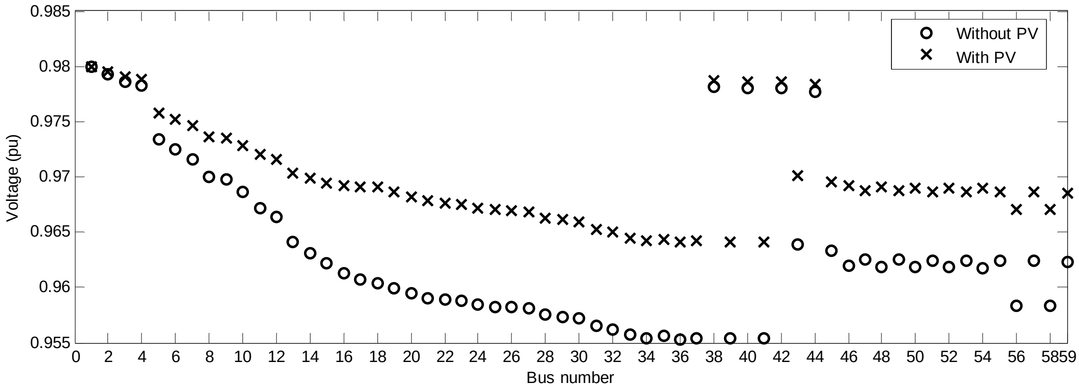

Figure 5.6: Voltage level comparison on the 59-bus system

Table 5.8: Voltage level compares between without DG and single DG

PEA system		Vmin (pu)	Vavg (pu)	Vmax (pu)
26 bus	Without DG	0.9767 (Bus no.23)	0.9777	0.9800
	Single DG	0.9776 (Bus no.23)	0.9785	0.9800
59 bus	Without DG	0.9758 (Bus no.36)	0.9839	0.9800
	Single DG	0.9641 (Bus no.36)	0.9699	0.9800

The benchmark population is 200 and the minimum value standard for the population is 50. Table 5.9 presents the optimal single DG (PV-type) placement by five PSO types with the population of 50. Fig. 5.7 and 5.8 show the convergence characteristic of real power loss minimization for the 26-bus and 59-bus radial distribution systems. The statistic variances of CPSO, PSO-TVIW, IRS-PSO, TVAC-PSO, and SHPSO-TVAC for optimal PV placement are presented in Table 5.10. The minimum value for the population has been chosen and the running results of the PSO model for 10 times are presented. The minimum power loss and calculation time are preferred. Fig. 5.9 shows the power loss between PV and without PV in a year. Fig. 5.10 shows the power reduction by PV in a year and Fig. 5.11 illustrated the power output by PV in a year. Table 5.11 shows the results of real single PV size considering solar radiation and total real power loss reduction on the 59-bus system of each month in a year, while Table 5.12 presents the PV benefits from both sides, i.e. PEA and the PV suppliers. The data would be useful for the policy makers who plan to install the PV power supply system.

Table 5.9: Optimal single DG placement by five PSO types (Population = 50)

Method	**Bus No.**	**DG size (MW)**	**Real power loss (kW)**	**Reactive power loss (kVAR)**	**Time (second)**
The total original loss in the 26 bus PEA			11.6925	26.0812	
GA [43]	14	6.9510	4.5500	10.1900	n/a
CPSO	14	6.4605	3.3387	10.2529	10.0620
PSO-TVIW	14	6.4468	3.3386	10.2571	8.5150
IRS-PSO	14	6.4460	***3.3386***	10.2573	8.7650
TVAC-PSO	14	6.4487	3.3386	10.2565	8.8440
SHPSO-TVAC	14	6.6725	3.3439	10.2052	8.8440
The total original loss in the 59 bus PEA			122.5559	278.8729	
GA [43]	18	9.0240	41.6200	91.7800	n/a
CPSO	18	8.9788	41.5715	91.6889	32.0620
PSO-TVIW	18	9.0119	***41.5704***	91.6779	28.3910
IRS-PSO	18	9.0746	41.5743	91.6705	28.4380
TVAC-PSO	18	9.0150	41.5704	91.6771	28.7340
SHPSO-TVAC	18	8.6549	41.6948	92.0550	28.3750

* n/a = not available

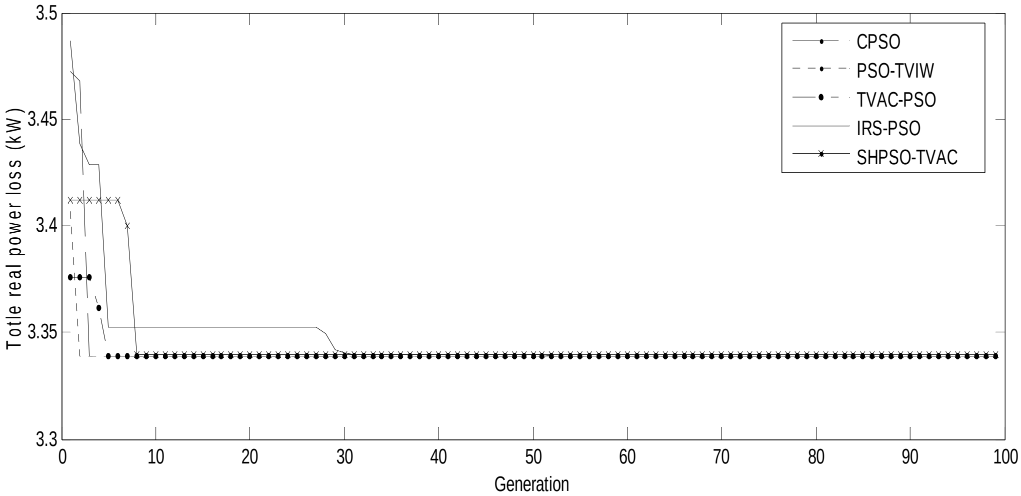

Figure 5.7: Convergence characteristics of real power loss minimization (26-bus system)

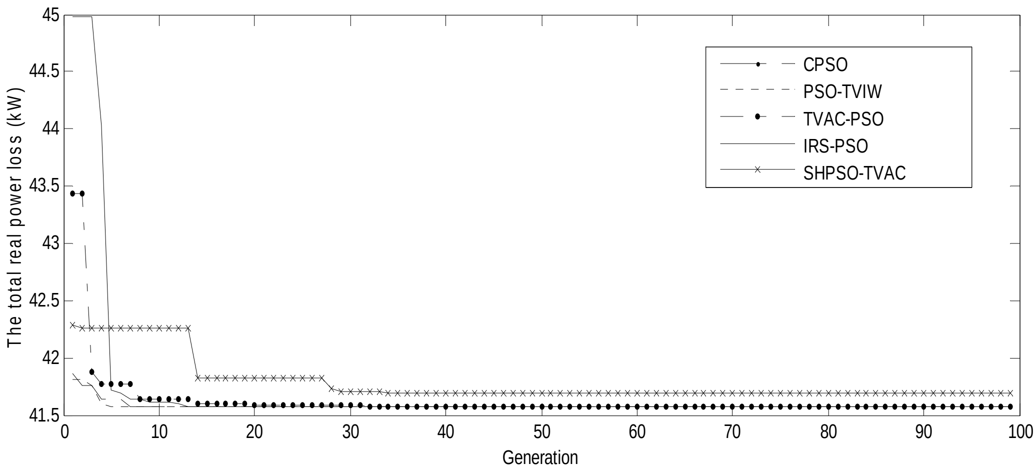

Figure 5.8: Convergence characteristics of real power loss minimization (59-bus system)

Table 5.10: The statistic variances of CPSO, PSO-TVIW, IRS-PSO, TVAC-PSO, and SHPSO-TVAC for optimal PV placement (pop = 50, run 10 times)

Method	**Considering factor**	**Maximum**	**Average**	**Minimum**
The 26 bus PEA				
CPSO	Ploss (kW)	3.3046	3.3390	3.3386
	Calculated time (sec)	10.672	9.1797	8.7190
PSO-TVIW	Ploss (kW)	***3.3386***	***3.3386***	***3.3386***
	Calculated time (sec)	***9.5940***	***8.6906***	***8.0160***
IRS-PSO	Ploss (kW)	***3.3386***	***3.3386***	***3.3386***
	Calculated time (sec)	10.047	8.9688	8.1720
TVAC-PSO	Ploss (kW)	***3.3386***	***3.3386***	***3.3386***
	Calculated time (sec)	9.7190	8.8501	8.1100
SHPSO-TVAC	Ploss (kW)	3.3538	3.3409	3.3386
	Calculated time (sec)	10.2981	8.9805	8.4060
The 59 bus PEA				
CPSO	Ploss (kW)	41.5789	41.6050	41.5704
	Calculated time (sec)	35.5790	30.1798	28.3130
PSO-TVIW	Ploss (kW)	***41.5704***	***41.5704***	***41.5704***
	Calculated time (sec)	38.6560	29.6877	***27.6410***
IRS-PSO	Ploss (kW)	41.5715	41.5706	41.5704
	Calculated time (sec)	29.9220	28.8547	28.1560
TVAC-PSO	Ploss (kW)	41.5743	41.5714	41.5704
	Calculated time (sec)	***29.5780***	28.6015	27.8590
SHPSO-TVAC	Ploss (kW)	41.6948	41.5983	41.5704
	Calculated time (sec)	28.9690	***28.4359***	27.9690

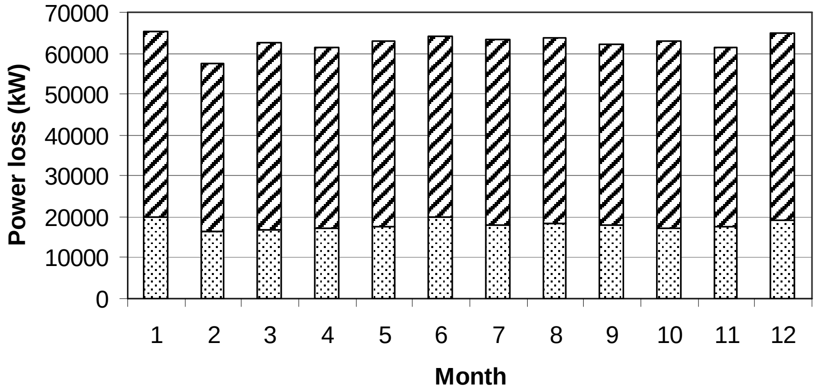

Figure 5.9: Power loss between PV and without PV in a year

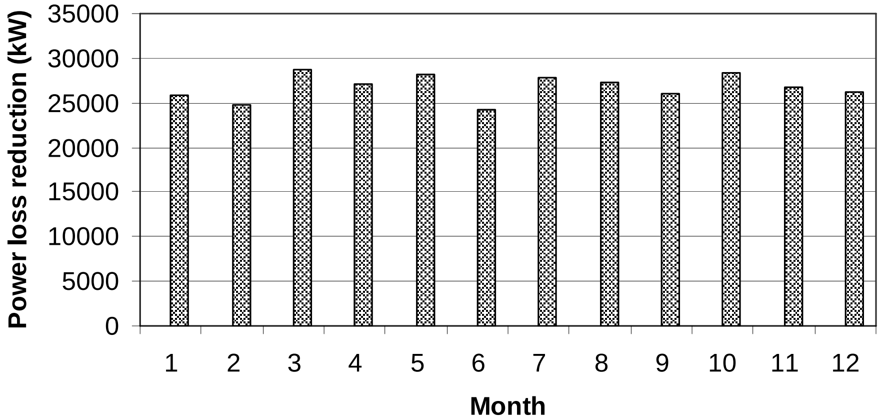

Figure 5.10: Power loss reduction by PV in a year

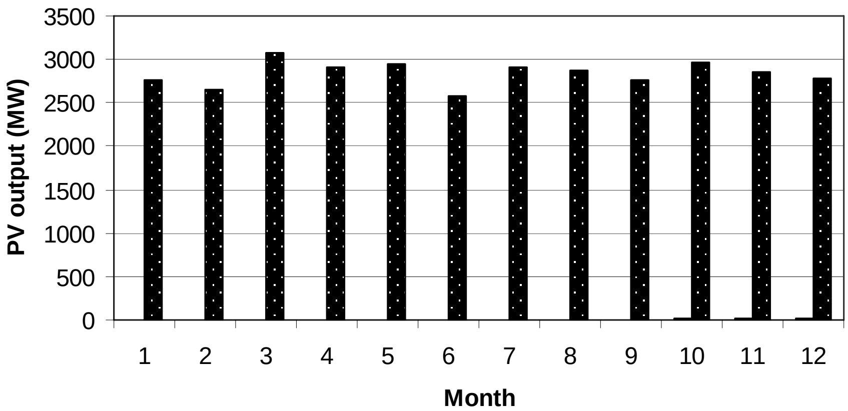

Figure 5.11: Power output by PV in a year

Table 5.11: Real single DG size (PV type) considering solar radiation and total real power loss reduction on the 59-bus system

January

Time	**6-7**	**7-8**	**8-9**	**9-10**	**10-11**	**11-12**	**12-13**	**13-14**	**14-15**	**15-16**	**16-17**	**17-18**
Global irradiance 15° (W/m2)	0.36	25.16	141.16	473.35	673.79	796.00	828.67	753.86	538.42	354.17	218.68	102.21
PV production (MW)	0.023	1.618	9.002	9.002	9.002	9.002	9.002	9.002	9.002	9.002	9.002	6.572
Ploss (kW)	121.84	95.71	41.57	41.57	41.57	41.57	41.57	41.57	41.57	41.57	41.57	47.41
Qloss (kW)	277.92	217.62	91.68	91.68	91.68	91.68	91.68	91.68	91.68	91.68	91.68	105.68
Vmax	0.980	0.980	0.980	0.980	0.980	0.980	0.980	0.980	0.980	0.980	0.980	0.980
Vavg	0.964	0.965	0.970	0.970	0.970	0.970	0.970	0.970	0.970	0.970	0.970	0.968
Vmin	0.955	0.957	0.964	0.964	0.964	0.964	0.964	0.964	0.964	0.964	0.964	0.962

February

Time	**6-7**	**7-8**	**8-9**	**9-10**	**10-11**	**11-12**	**12-13**	**13-14**	**14-15**	**15-16**	**16-17**	**17-18**
Global irradiance 15° (W/m2)	6.73	130.83	204.34	442.79	603.79	786.11	649.58	783.98	494.03	352.96	269.65	79.39
PV production (MW)	0.433	8.412	9.002	9.002	9.002	9.002	9.002	9.002	9.002	9.002	9.002	5.105
Ploss (kW)	114.63	41.92	41.57	41.57	41.57	41.57	41.57	41.57	41.57	41.57	41.57	56.58
Qloss (kW)	261.28	92.64	91.68	91.68	91.68	91.68	91.68	91.68	91.68	91.68	91.68	127.08
Vmax	0.980	0.980	0.980	0.980	0.980	0.980	0.980	0.980	0.980	0.980	0.980	0.980
Vavg	0.964	0.970	0.970	0.970	0.970	0.970	0.970	0.970	0.970	0.970	0.970	0.967
Vmin	0.956	0.964	0.964	0.964	0.964	0.964	0.964	0.964	0.964	0.964	0.964	0.960

Table 5.11: Real single DG size (PV type) considering solar radiation and total real power loss reduction on the 59-bus system (Continued)

March

Time	**6-7**	**7-8**	**8-9**	**9-10**	**10-11**	**11-12**	**12-13**	**13-14**	**14-15**	**15-16**	**16-17**	**17-18**
Global irradiance 15° (W/m2)	35.65	129.84	162.10	371.93	493.38	618.68	677.91	719.52	494.92	457.61	267.53	114.41
PV production (MW)	2.292	8.349	9.002	9.002	9.002	9.002	9.002	9.002	9.002	9.002	9.002	7.357
Ploss (kW)	86.22	42.00	41.57	41.57	41.57	41.57	41.57	41.57	41.57	41.57	41.57	44.25
Qloss (kW)	195.71	92.83	91.68	91.68	91.68	91.68	91.68	91.68	91.68	91.68	91.68	98.25
Vmax	0.980	0.980	0.980	0.980	0.980	0.980	0.980	0.980	0.980	0.980	0.980	0.980
Vavg	0.965	0.969	0.970	0.970	0.970	0.970	0.970	0.970	0.970	0.970	0.970	0.969
Vmin	0.958	0.963	0.964	0.964	0.964	0.964	0.964	0.964	0.964	0.964	0.964	0.963

April

Time	**6-7**	**7-8**	**8-9**	**9-10**	**10-11**	**11-12**	**12-13**	**13-14**	**14-15**	**15-16**	**16-17**	**17-18**
Global irradiance 15° (W/m2)	20.64	145.39	227.18	366.35	593.87	777.85	866.17	669.44	457.99	300.89	176.16	85.21
PV production (MW)	1.327	9.002	9.002	9.002	9.002	9.002	9.002	9.002	9.002	9.002	9.002	5.479
Ploss (kW)	100.08	41.57	41.57	41.57	41.57	41.57	41.57	41.57	41.57	41.57	41.57	53.84
Qloss (kW)	227.71	91.68	91.68	91.68	91.68	91.68	91.68	91.68	91.68	91.68	91.68	120.69
Vmax	0.980	0.980	0.980	0.980	0.980	0.980	0.980	0.980	0.980	0.980	0.980	0.980
Vavg	0.965	0.970	0.970	0.970	0.970	0.970	0.970	0.970	0.970	0.970	0.970	0.968
Vmin	0.957	0.964	0.964	0.964	0.964	0.964	0.964	0.964	0.964	0.964	0.964	0.961

Table 5.11: Real single DG size (PV type) considering solar radiation and total real power loss reduction on the 59-bus system (Continued)

May

Time	**6-7**	**7-8**	**8-9**	**9-10**	**10-11**	**11-12**	**12-13**	**13-14**	**14-15**	**15-16**	**16-17**	**17-18**
Global irradiance 15° (W/m2)	40.20	90.29	325.97	358.53	516.24	599.73	334.67	480.71	501.92	433.58	230.37	84.15
PV production (MW)	2.585	5.805	9.002	9.002	9.002	9.002	9.002	9.002	9.002	9.002	9.002	5.411
Ploss (kW)	82.39	51.67	41.57	41.57	41.57	41.57	41.57	41.57	41.57	41.57	41.57	54.31
Qloss (kW)	186.87	115.64	91.68	91.68	91.68	91.68	91.68	91.68	91.68	91.68	91.68	121.80
Vmax	0.980	0.980	0.980	0.980	0.980	0.980	0.980	0.980	0.980	0.980	0.980	0.980
Vavg	0.965	0.968	0.970	0.970	0.970	0.970	0.970	0.970	0.970	0.970	0.970	0.967
Vmin	0.958	0.961	0.964	0.964	0.964	0.964	0.964	0.964	0.964	0.964	0.964	0.961

June

Time	**6-7**	**7-8**	**8-9**	**9-10**	**10-11**	**11-12**	**12-13**	**13-14**	**14-15**	**15-16**	**16-17**	**17-18**
Global irradiance 15° (W/m2)	43.35	149.70	351.62	466.85	744.26	745.20	666.74	104.35	234.50	141.66	19.27	12.86
PV production (MW)	2.788	9.002	9.002	9.002	9.002	9.002	9.002	9.002	9.002	9.002	1.239	0.827
Ploss (kW)	79.84	41.57	41.57	41.57	41.57	41.57	41.57	41.57	41.57	41.57	101.45	108.01
Qloss (kW)	180.97	91.68	91.68	91.68	91.68	91.68	91.68	91.68	91.68	91.68	230.87	246.03
Vmax	0.980	0.980	0.980	0.980	0.980	0.980	0.980	0.980	0.980	0.980	0.980	0.980
Vavg	0.966	0.970	0.970	0.970	0.970	0.970	0.970	0.970	0.970	0.970	0.967	0.964
Vmin	0.958	0.964	0.964	0.964	0.964	0.964	0.964	0.964	0.964	0.964	0.957	0.956

Table 5.11: Real single DG size (PV type) considering solar radiation and total real power loss reduction on the 59-bus system (Continued)

July

Time	**6-7**	**7-8**	**8-9**	**9-10**	**10-11**	**11-12**	**12-13**	**13-14**	**14-15**	**15-16**	**16-17**	**17-18**
Global irradiance 15° (W/m2)	26.79	92.25	204.49	300.35	239.76	594.88	732.53	566.57	523.53	444.54	338.88	83.43
PV production (MW)	1.722	5.932	9.002	9.002	9.002	9.002	9.002	9.002	9.002	9.002	9.002	5.364
Ploss (kW)	94.17	50.88	41.57	41.57	41.57	41.57	41.57	41.57	41.57	41.57	41.57	54.65
Qloss (kW)	214.09	113.81	91.68	91.68	91.68	91.68	91.68	91.68	91.68	91.68	91.68	122.58
Vmax	0.980	0.980	0.980	0.980	0.980	0.980	0.980	0.980	0.980	0.980	0.980	0.980
Vavg	0.965	0.968	0.970	0.970	0.970	0.970	0.970	0.970	0.970	0.970	0.970	0.967
Vmin	0.957	0.961	0.964	0.964	0.964	0.964	0.964	0.964	0.964	0.964	0.964	0.961

August

Time	**6-7**	**7-8**	**8-9**	**9-10**	**10-11**	**11-12**	**12-13**	**13-14**	**14-15**	**15-16**	**16-17**	**17-18**
Global irradiance 15° (W/m2)	18.12	62.79	173.81	246.43	244.46	255.85	609.27	653.33	515.48	418.12	212.57	101.33
PV production (MW)	1.165	4.037	9.002	9.002	9.002	9.002	9.002	9.002	9.002	9.002	9.002	6.515
Ploss (kW)	102.60	65.96	41.57	41.57	41.57	41.57	41.57	41.57	41.57	41.57	41.57	47.68
Qloss (kW)	233.53	148.83	91.68	91.68	91.68	91.68	91.68	91.68	91.68	91.68	91.68	106.32
Vmax	0.980	0.980	0.980	0.980	0.980	0.980	0.980	0.980	0.980	0.980	0.980	0.980
Vavg	0.964	0.967	0.970	0.970	0.970	0.970	0.970	0.970	0.970	0.970	0.970	0.968
Vmin	0.957	0.959	0.964	0.964	0.964	0.964	0.964	0.964	0.964	0.964	0.964	0.962

Table 5.11: Real single DG size (PV type) considering solar radiation and total real power loss reduction on the 59-bus system (Continued)

September

Time	**6-7**	**7-8**	**8-9**	**9-10**	**10-11**	**11-12**	**12-13**	**13-14**	**14-15**	**15-16**	**16-17**	**17-18**
Global irradiance 15° (W/m2)	21.12	210.93	309.78	365.85	648.93	425.50	529.48	435.93	170.05	139.28	107.50	41.30
PV production (MW)	1.358	9.002	9.002	9.002	9.002	9.002	9.002	9.002	9.002	8.955	6.912	2.655
Ploss (kW)	99.61	41.57	41.57	41.57	41.57	41.57	41.57	41.57	41.57	41.57	45.89	81.49
Qloss (kW)	226.64	91.68	91.68	91.68	91.68	91.68	91.68	91.68	91.68	91.70	102.12	184.79
Vmax	0.980	0.980	0.980	0.980	0.980	0.980	0.980	0.980	0.980	0.980	0.980	0.980
Vavg	0.965	0.970	0.970	0.970	0.970	0.970	0.970	0.970	0.970	0.970	0.969	0.966
Vmin	0.957	0.964	0.964	0.964	0.964	0.964	0.964	0.964	0.964	0.964	0.962	0.958

October

Time	**6-7**	**7-8**	**8-9**	**9-10**	**10-11**	**11-12**	**12-13**	**13-14**	**14-15**	**15-16**	**16-17**	**17-18**
Global irradiance 15° (W/m2)	22.27	131.42	279.28	629.33	750.62	490.69	682.27	448.44	718.10	441.23	294.46	74.15
PV production (MW)	1.432	8.450	9.002	9.002	9.002	9.002	9.002	9.002	9.002	9.002	9.002	4.768
Ploss (kW)	98.48	41.88	41.57	41.57	41.57	41.57	41.57	41.57	41.57	41.57	41.57	59.29
Qloss (kW)	224.03	92.53	91.68	91.68	91.68	91.68	91.68	91.68	91.68	91.68	91.68	133.38
Vmax	0.980	0.980	0.980	0.980	0.980	0.980	0.980	0.980	0.980	0.980	0.980	0.980
Vavg	0.965	0.970	0.970	0.970	0.970	0.970	0.970	0.970	0.970	0.970	0.970	0.987
Vmin	0.957	0.964	0.964	0.964	0.964	0.964	0.964	0.964	0.964	0.964	0.964	0.960

Table 5.11: Real single DG size (PV type) considering solar radiation and total real power loss reduction on the 59-bus system (Continued)

November

Time	**6-7**	**7-8**	**8-9**	**9-10**	**10-11**	**11-12**	**12-13**	**13-14**	**14-15**	**15-16**	**16-17**	**17-18**
Global irradiance 15° (W/m2)	32.70	228.69	476.45	696.71	703.23	713.46	554.04	351.33	328.77	349.14	230.93	46.38
PV production (MW)	2.102	9.002	9.002	9.002	9.002	9.002	9.002	9.002	9.002	9.002	9.002	2.982
Ploss (kW)	88.8	41.57	41.57	41.57	41.57	41.57	41.57	41.57	41.57	41.57	41.57	77.47
Qloss (kW)	201.7	91.68	91.68	91.68	91.68	91.68	91.68	91.68	91.68	91.68	91.68	175.5
Vmax	0.98	0.98	0.98	0.98	0.98	0.98	0.98	0.98	0.98	0.98	0.98	0.98
Vavg	0.965	0.97	0.97	0.97	0.97	0.97	0.97	0.97	0.97	0.97	0.97	0.966
Vmin	0.957	0.964	0.964	0.964	0.964	0.964	0.964	0.964	0.964	0.964	0.964	0.958

December

Time	**6-7**	**7-8**	**8-9**	**9-10**	**10-11**	**11-12**	**12-13**	**13-14**	**14-15**	**15-16**	**16-17**	**17-18**
Global irradiance 15° (W/m2)	3.45	91.98	174.03	407.07	490.89	763.55	801.92	735.68	495.70	234.49	226.60	42.45
PV production (MW)	0.222	5.914	9.002	9.002	9.002	9.002	9.002	9.002	9.002	9.002	9.002	2.730
Ploss (kW)	118.30	50.99	41.57	41.57	41.57	41.57	41.57	41.57	41.57	41.57	41.57	80.56
Qloss (kW)	269.75	114.06	91.68	91.68	91.68	91.68	91.68	91.68	91.68	91.68	91.68	182.64
Vmax	0.980	0.980	0.980	0.980	0.980	0.980	0.980	0.980	0.980	0.980	0.980	0.980
Vavg	0.964	0.968	0.970	0.970	0.970	0.970	0.970	0.970	0.970	0.970	0.970	0.966
Vmin	0.956	0.961	0.964	0.964	0.964	0.964	0.964	0.964	0.964	0.964	0.964	0.958

Table 5.12: Summary of PV benefits

Summary of PV benefits		
PEA		
Average real power loss reduction per year	321.05	MW per year
PV supplier		
PV output	34,066.75	MW per year

5.4 Conclusion

The results of applying PSO algorithm to the optimal allocation of DG in distribution networks were presented. The effectiveness of the proposed algorithm in solving DG allocation problem was demonstrated through a numerical example. Distribution feeder of PEA distribution networks were solved by means of the proposed algorithm. The results of the algorithm revealed the superior characteristics of the PSO.

Chapter 6

Contributions of The Study

This chapter aims to present the contributions of the study. The new concept of PSO model and results are addressed. This study proposes self-organizing hierarchical binary particle swarm optimization with time varying acceleration coefficient (SHBPSO-TVAC) for solving optimal number and size of photovoltaic (PV) unit placement on a radius system. For optimal number of PV unit problem, SHBPSO is used to have quick convergence and explore solution space in the new direction. For optimal sizes of PV unit problem, SHBPSO-TVAC is used to avoid local optimum trap. The objective is to minimize total real power loss with solar irradiance capability in Thailand. Multiple PV unit grid connected systems are considered. SHBPSO-TVAC can find better locations and sizes than other methods i.e. the classical binary PSO (CBPSO), the binary PSO with time varying inertia weight (BPSO-TVIW), the binary PSO with time varying acceleration coefficients (BPSO-TVAC) and the binary PSO with sigmoid increasing inertia weight (BPSO-SIIW) on the 59-bus radial distributed system. The results are analyzed including real power of PV supplies into the system with different time to be investment benefits and total yearly power loss reduction.

6.1 Introduction

Optimal photovoltaic distributed generation (PV-DG) placement, a mixed integer problem, has been solved by various methods including genetic algorithm (GA) [44-46], the improved reinitialized social structure particle swarm optimization (IRS-PSO) [47], and the multi-objective particle swarm optimization (MOPSO) [48-50]. Moreover, the total power loss is considered to be one of the objective functions. For instance, the optimal DG placement proposed by Hedayati and Nabaviniaki [44] was to minimize the total real power loss by simple GA method. However, it is applicable to only one DG. Prommee and Ongsakul [47] proposed the optimal multiple DGs placement in a microgrid system by improved reinitialized social structure particle swarm optimization to minimize the total real power loss. However, IRS-PSO can not find optimal number of DG because of the fitness distance ratio limitation. Binary programming proposed by Cai et al. [50] optimized two objective functions including economic and environmental profit to find the optimal design of photovoltaic grid connected systems in single DG. However, the total power loss minimization and solar irradiance capability were not considered. Binary PSO is improved for unit commitment problem in Yuan et al. [51] by adding sigmoid increasing inertia weight (SIIW) to improve the performance of PSO. Moreover, the inertia weight of binary PSO is a tool to control the exploration and exploitation abilities of the swarm. For four nonlinear benchmark functions, SIIW can give better performance than linear decreasing inertia weight (LDIW), linear increasing inertia weight (LIIW) and sigmoid decreasing inertia weight (SDIW) [51]. However, the SIIW calculation time is too long for finding a stable sigmoid constant in the weight equation.

In this study, a self-organizing hierarchical binary particle swarm optimization with time varying acceleration coefficient (SHBPSO-TVAC) is proposed to find optimal number and size of PV placement to minimize total real power loss and increase voltage level. The binary PSO is improved by TVAC for roaming individually through a wide search space and SHPSO-TVAC can avoid the local trap and explore new areas. In SHBPSO-TVAC method, binary PSO is used to find optimal number of PV placement and SHPSO-TVAC is applied for optimal PV size. Moreover, the solar irradiance in Thailand is also considered in this study. The SHBPSO-TVAC solutions are compared with CBPSO, BPSO-TVIW, BPSO-TVAC and BPSO-SIIW on the 59-bus radial distributed system.

6.2 Problem Formulation

Size and location of PV units are crucial factors in the application of PV very small scale power producer (PV-VSPP) for its maximum benefits. In the present study, the binary PSO based techniques have been proposed and an attempt has been made to determine optimal PV size for minimizing real power losses in a radial distribution network.

6.2.1 Objective Function

The power loss reduction in a distribution system is required for efficient power system operation. The difference between the generated power and the demand will give the loss. The objective function is designed to reduce power loss which can be defined as equation (6.1).

$$\text{Minimize} \qquad P_{loss} = \sum_{k=1}^{N_{SC}} Loss_k \tag{6.1}$$

The total real power loss equation can be calculated by equation (6.2) [47].

$$P_{loss} = \sum_{i=1}^{n}\sum_{j=1}^{n} A_{ij}(P_iP_j + Q_iQ_j) + B_{ij}(Q_iP_j - P_iQ_j) \tag{6.2}$$

where

$$A_{ij} = \frac{R_{ij}\cos\left(\delta_i - \delta_j\right)}{V_iV_j} \tag{6.3}$$

$$B_{ij} = \frac{R_{ij}\sin\left(\delta_i - \delta_j\right)}{V_iV_j} \tag{6.4}$$

Subject to the constraints as described in equations (6.5) to (6.7) [33].

$$\text{Power balance constraints:} \qquad \sum_{i=1}^{N} P_{PV,i} = \sum_{i=1}^{N} P_{D,i} + P_{loss} \tag{6.5}$$

Voltage limits: $$0.95pu \le |V_i| \le 1.10pu \tag{6.6}$$

Note that the PEA voltage standard is between 0.95 and 1.10 per unit. In load flow calculation, the voltage level of the slake bus is set at 0.98 per unit. The real power generation limits are set as equation (6.7).

Real power generation limits: $$0.05MW \le P_{PV,i} \le 5MW \tag{6.7}$$

6.2.2 PV Power Function

The photovoltaic system produces only real power. The SHBPSO-TVAC will search for optimal real power size of PV unit *i* ($P_{PV,i}$) and its location. If a PV of size $P_{PV,i}$ is installed at bus *i*, the net power of bus *i* can be calculated by equation (6.8) [47].

$$P_i = P_{PV,i} - P_{D,i} \tag{6.8}$$

Rahman and Yamashiro [52] noted that the PV distributed generation system can be run to get maximum benefit by selling all PV output power to the grid line. In this study, when PV power is available during daytime (about 6:00 to 18:00) the load demand is fulfilled by the PV power and a preset amount of buy power. In the rest of a day, there is insufficient of PV power during nighttime (about 18:00 to 6:00), a sufficient amount of buy power is taken to meet the load demand. Therefore, the system uses 100% of PV output to provide maximum benefit. Moreover, Eltawil and Zhao [53] illustrated that PV distribution systems provide financial benefit in two ways: one is by generating power from PV energy and the other is by using the clean power instead of the fossil fuels.

6.2.3 Solar Irradiance in Thailand

PV production is becoming increasingly important as solar produced energy is growing strongly. Within the next few years the share of solar produced energy injected on power grids during peak hours will become noticeable in Thailand which is a tropical country and has plenty of sunshine. Especially the country legislation encourages the deployment of increasingly large PV power plants.

Hourly global solar irradiance is very important for designing PV systems. However, it is observed at a limited number of meteorological stations in Thailand. Chupong and Plangklang [54] noted that a significant limitation of PV system is the uncertainty of power from the sun. For the purpose of solar energy utilization, the values of global irradiance at a particular location are therefore essential for the design and efficient operation of the system.

Table 6.1 presents the average global irradiance in a measure unit of W/m^2 on the array plane with 15 degree inclination angle. This data were measured at Asian Institute of Technology meteorological station in Thailand (latitude 14.06°N and longitude 100.65°E) [55]. For a fixed tilt angle, the maximum power over the course of a year is obtained when the tilt angle is equal to the latitude of the location [56]. The irradiance depends on the season, the position of the sun in the sky and the weather. The hourly power output of PV grid connected system can be evaluated by using the measured hourly global irradiance data.

Table 6.1: Average global solar irradiance at AIT meteorological station, Thailand

Month	am						noon	pm				
	6.00-7.00	7.00-8.00	8.00-9.00	9.00-10.00	10.00-11.00	11.00-12.00	12.00-1.00	1.00-2.00	2.00-3.00	3.00-4.00	4.00-5.00	5.00-6.00
January	0.36	25.16	141.16	473.35	673.79	796.00	828.67	753.86	538.42	354.17	218.68	102.21
February	6.73	130.83	204.34	442.79	603.79	786.11	649.58	783.98	494.03	352.96	269.65	79.39
March	35.65	29.84	162.10	371.93	493.38	618.68	677.91	719.52	494.92	457.61	267.53	114.41
April	20.64	145.39	227.18	366.35	593.87	777.85	866.17	669.44	457.99	300.89	176.16	85.21
May	40.20	90.29	325.97	358.53	516.24	599.73	334.67	480.71	501.92	433.58	230.37	84.15
June	43.35	149.70	351.62	466.85	744.26	745.20	666.74	104.35	234.50	141.66	19.27	12.86
July	26.79	92.25	204.49	300.35	239.76	594.88	732.53	566.57	523.53	444.54	338.88	83.43
August	18.12	62.79	173.81	246.43	244.46	255.85	609.27	653.33	515.48	418.12	212.57	101.33
September	21.12	210.93	309.78	365.85	648.93	425.50	529.48	435.93	170.05	139.28	107.50	41.30
October	22.27	131.42	279.28	629.33	750.62	490.69	682.27	448.44	718.10	441.23	294.46	74.15
November	32.70	228.69	476.45	696.71	703.23	713.46	554.04	351.33	328.77	349.14	230.93	46.38
December	3.45	91.98	174.03	407.07	490.89	763.55	801.92	735.68	495.70	234.49	226.60	42.45

6.3 Improved Binary PSO for Optimal PV Placement Algorithm

The PSO is a population based stochastic optimization algorithm [37]. The element of a population is called “particles”. The particles represent PV sizes and locations for optimal PV placement.

6.3.1 Classical Binary PSO

Classical PSO (CPSO) is the original PSO approach and it is the base model for many improved PSO versions. The classical PSO mathematical model proposed by James Kennedy (social-psychologist) and Russell Eberhart (electrical engineer) [16] consists of two main equations: velocity and position update equations which expressed as equations (6.9) and (6.10). In this study, CPSO is used for optimal PV size.

$$v_{i=1to|l|,pop}^{k+1} = v_{i,pop}^{k} + C_p R_1 (p_{i,pop}^{k} - x_{i,pop}^{k}) + C_g R_2 (g_{pop}^{k} - x_{i,pop}^{k}) \tag{6.9}$$

$$x_{i=1to|l|,pop}^{k+1} = x_{i=1to|l|,pop}^{k} + v_{i=1to|l|,pop}^{k+1} \tag{6.10}$$

For classical binary PSO (CBPSO), it is used for optimal number of PV units. Binary PSO has no position update equation. Fig. 1 shows the sigmoid function. The velocity value is mapped with interval 0 to 1, which is given as equation (6.11) [57].

$$x_{i=1to|l|,pop}^{k+1} = \begin{cases} 1, & rand(1) < s(v^{k+1}) \\ 0, & otherwise \end{cases} \tag{6.11}$$

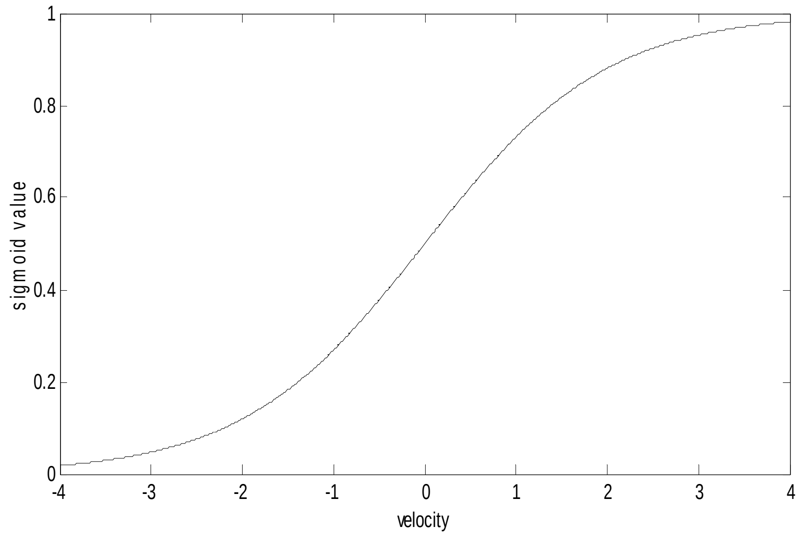

Figure 6.1: Sigmoid function
[57]

6.3.2 Binary PSO with Time Varying Inertia Weight

Binary PSO with time varying inertia weight (BPSO-TVIW) has been proposed by Shi and Eberhart [36,37], the method is updated to improve the location search precision by adding weight, the velocity is updated as equation (6.12) and the weight function is given as equation (6.13).

$$v_{i=1to|I|,pop}^{k+1} = w^k v_{i,pop}^k + C_p R_1 (p_{i,pop}^k - x_{i,pop}^k) + C_g R_2 (g_{pop}^k - x_{i,pop}^k) \tag{6.12}$$

$$w^k = w_{\max} - \left(\frac{w_{\max} - w_{\min}}{k_{\max}} \right) k \tag{6.13}$$

The maximum and minimum weight values, $w_{\max}$ and $w_{\min}$ are set as 0.9 and 0.4, respectively.

6.3.3 Binary PSO with Time Varying Acceleration Coefficients

PSO with time varying acceleration coefficients (TVAC-PSO) is an extensive version from PSO-TVIW proposed by Suganthan [39]. In the initial stages of the search of TVAC-PSO, particles are encouraged to roam individually through a wide search space. This is with a high acceleration factor of the cognitive component and a less acceleration factor of the social component in equation (6.12). The time varying acceleration coefficients of the cognitive and social components are determined by equations (6.14) and (6.15) [58]. In this study, TVAC-PSO becomes to be BPSO-TVAC use for optimal number of PV units. Normally, the acceleration coefficients are in the range of 0.5 to 2.5 [39].

$$C_p = C_{p,i} - \left(\frac{C_{p,i} - C_{p,f}}{k_{\max}} \right) k \tag{6.14}$$

$$C_g = C_{g,i} - \left(\frac{C_{g,i} - C_{g,f}}{k_{\max}} \right) k \tag{6.15}$$

6.3.4 Binary PSO with Sigmoid Increasing Inertia Weight

Binary PSO is used for optimal number of PV units. Generally, the sigmoid inertia weight of BPSO-TVIW starts from 0.9 linearly decreasing to 0.4. On the other hand, the sigmoid function is a nonlinear function which is mismatch with linear inertia weight. As a result, the PSO convergence rate is slow. Sigmoid increasing inertia weight (SIIW) is added into the sigmoid function to give a better performance.

The present study proposes a new nonlinear function modulated inertia weight adaptation with time for improved performance of PSO algorithm. Instead of linearly increasing of inertia weight, the schema attempted to increase inertia weight by means of sigmoid function, as shown in Fig. 6.2. Increasing inertia weight equation is given as equation (6.16) [57].

$$w^k = \frac{(w_{start} - w_{end})}{(1 + e^{u*(k-n*gen)})} + w_{end} \tag{6.16}$$

where

$$u = 10^{(\log(gen)-2)} \tag{6.17}$$

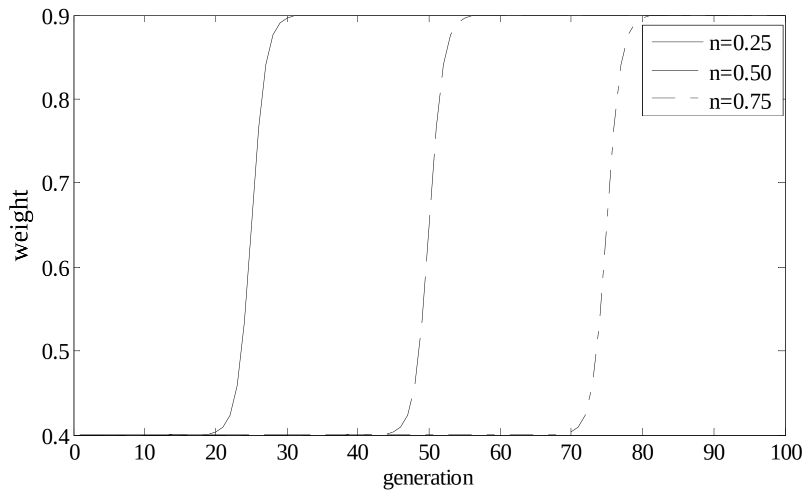

Figure 6.2: Sigmoid increasing inertia weight [57]

6.3.5 Self-Organizing Hierarchical Binary PSO with Time Varying Acceleration Coefficients

Self-organizing hierarchical binary PSO with time varying acceleration coefficient (SHBPSO-TVAC) is a novel PSO that preserves the effectiveness of TVAC-PSO for roaming towards the search space at the beginning [42]. Boonchuay and Ongsakul [40] noted that the previous velocity term is made to zero to rush towards a local optimum solution. However, with this modification, particles lose the momentum to find better solutions in the later stage of the search. SHBPSO-TVAC can overcome this weakness by reinitialized the velocity vector of a particle whenever it stagnates during the search and given as equation (6.18) [41].

If $v_{id} = 0$ and $R_3 < 0.5$ then

$v_{id} = R_4 \times v_{d,\max}$

else $v_{id} = -R_5 \times v_{d,\max}$

$$v_{d,\max} = \left(\frac{x_{d,\max} - x_{d,\min}}{R} \right) \tag{6.18}$$

In this study, the binary PSO is improved to be SHBPSO-TVAC to find the optimal number of PV units. The proposed method using SHBPSO-TVAC can be described in nine steps as follows.

Step 1: Input parameters of the system and PSO.
The number of bus, line impedance and load are the required database.
The PSO parameters are different and depend on PSO types.

Step 2: Initialize 50 particles with random position and zero velocity.
$x_{i,l}^{k}$ = {1 0 1 0 0 0 0 1……1} = {2 0 5 0 0 0 0 15……59}
$x_{i,s}^{k}$ = {2.1480 1.7782 0.3558 0.6688 1.2225 ……} MW.

Step 3: Set the generation counter g=1.

Step 4: Evaluate the objective value as the total real power loss by Backward-Forward Sweep load flow method.

Step 5: Update the personal best (pbest) and the global best (gbest).

Step 6: Update and reinitialize velocity by equation (6.18)
Update position by equation (6.11) for optimal number of PV units and using equation (6.14) for optimal PV size.

Step 7: If the generation counter reaches 100, go to step 9.
Otherwise, go to the next step.

Step 8: Update the generation counter g=g+1, return to step 4.

Step 9: The global best solution of PSO will show the optimal number and size of multi-PV units.

In Backward-Forward Sweep load flow method, branch current is initially calculated. Prommee and Ongsakul [17] noted that during each backward sweep process the voltage obtained at forward sweep is kept constant and updated branch currents are sent backward along the feeder using backward path. In the forward sweep, the values of current from forward sweep are kept as constant and the voltage of each node will be updated. The feeder substation voltage is kept constant. The backward and forward sweep will be repeated until a stopping criterion is met by measuring the voltage mismatch after the completion of one round of backward and forward sweep. Voltage in each node and current in branch will be used to find the real and reactive power loss of the distribution system. Only the best location and the size will be recorded to guarantee a better future value in the best fitness database. Subsequently, the remaining locations and PV sizes will be randomly generated again. The flowchart of SHBPSO-TVAC for solving optimal PV placement is shown in Fig. 6.3.

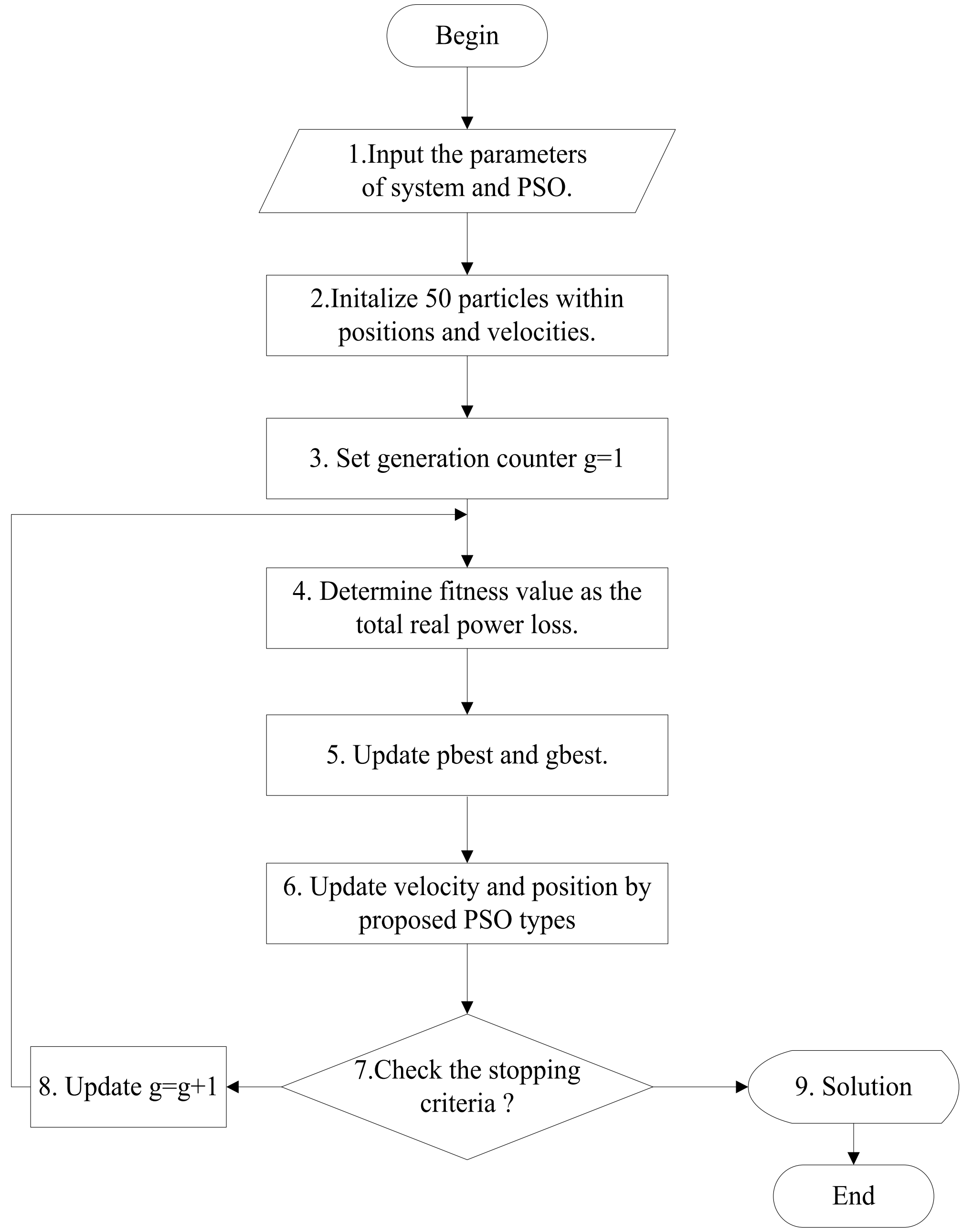

Figure 6.3: Flowchart of SHBPSO-TVAC for optimal PV placement

6.4 Numerical Results of the Proposed Binary PSO Method

To validate the applicability of the proposed method, the PEA distribution network in Ayutthaya province is utilized as the test system. Fig. 6.4 shows the single line diagram of the 59-bus distribution system. The system has the total load of 12.17 MW and 6.71 MVAR. The bus number 1 is connected by utility and the total original real and reactive power losses of the system are 122.49 kW and 279.41 kVAR, respectively.

When multiple small PV units are optimally placed, the bus voltage limits are set to 0.95 and 0.98 per unit, and the real power generation limits are set to 0.05 and 5 MW. In the test system, bus 1 has been considered the slack bus and is not considered for the PV placement.

Set of allowable PV locations (l)

$$l = \{2, 3, 4, 5, 6, \ldots\ldots., 57, 58, 59\}$$

In Table 6.2, the inertia weight and the acceleration coefficients of different PSO approaches are given. In CBPSO, the weight is kept constant at one, and the cognitive and the social coefficients are usually kept constant at two. In BPSO–TVIW, the weight is linearly decreased from 0.9 to 0.4, and the acceleration coefficients are similar to CBPSO. In BPSO–TVAC, the acceleration coefficients are varied. The coefficient of cognitive component is decreased in the range of 2.5–0.5 while the social learning factor is increased from 0.5 to 2.5 [41]. In BPSO-SIIW, the inertia weight at the start is set at 0.4 and the inertia weight at the end is set at 0.9. Different sigmoid constant are used, that are: 0.25, 0.5 and 0.75. The weight is linearly increased from 0.4 to 0.9, and the acceleration coefficients are similar to CBPSO and BPSO–TVIW. Finally, in SHBPSO–TVAC, the velocity term is neglected, thus the weight is made to zero, and the rest components are similar to BPSO–TVAC.

Tables 6.3 presents the results of a binary PSO based algorithm to the optimal allocation of multiple PV units minimizing real power loss in the distribution network. The effectiveness of the proposed algorithm in solving PV allocation problem has been demonstrated on distribution test feeders having 59 buses. The results on the proposed binary PSO based algorithm methods provide solutions for optimal size and allocation of multiple PV placement problems.

The decrease in total real power loss depends on the location and size of PV units. It is obvious that installation of PV units leads to reduction in total power losses. As shown in Tables 6.4, SHBPSO-TVAC total losses are much less than other methods, i.e. CBPSO, BPSO-TVIW, BPSO-TVAC and BPSO-SIIW. Moreover, SHBPSO-TVAC gives the minimum loss for both real and reactive powers. SHBPSO-TVAC can reduce loss by 75.94%. Apparently, the SHBPSO-TVAC is the best method for optimal placement because of minimum real power loss.

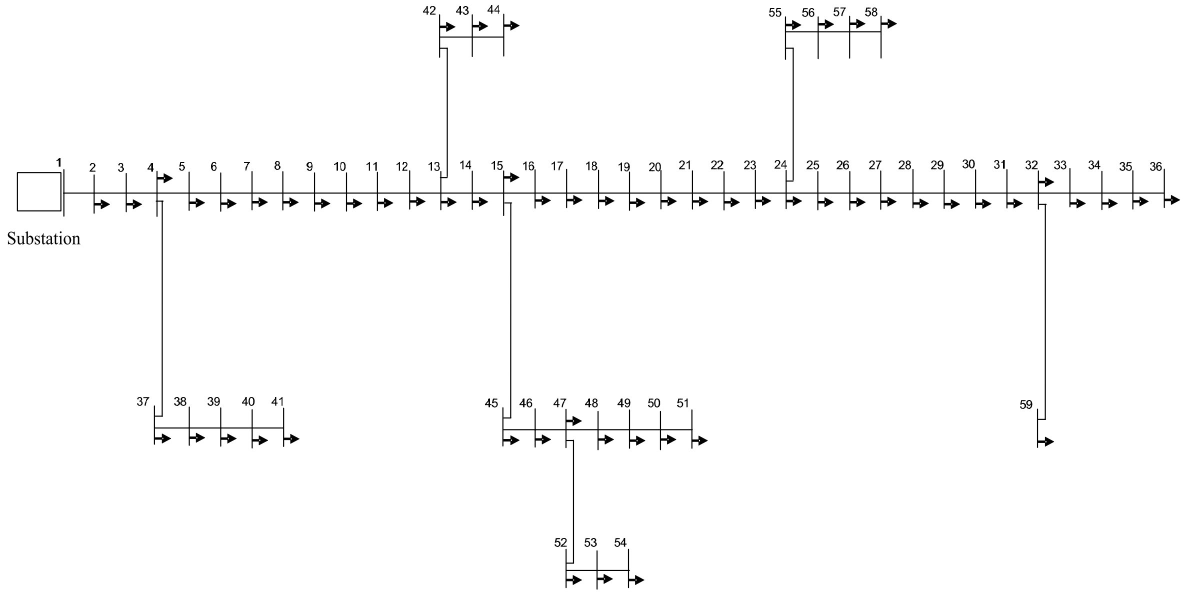

Figure 6.4: Single line diagram of the 59-bus distribution system

Table 6.2: Coefficients of different PSO approaches

Method	*SIIW*				C_p	C_g
	w_{start}	w_{end}	n	w	$\left(C_{p,i} - C_{p,f}\right)$	$\left(C_{g,i} - C_{g,f}\right)$
CBPSO	-	-	-	1	2	2
BPSO-TVIW	-	-	-	Decreasing (0.9-0.4)	2	2
BPSO-TVAC	-	-	-	Decreasing (0.9-0.4)	Decreasing (2.5-0.5)	Increasing (0.5-2.5)
BPSO-SIIW	0.4	0.9	0.25 0.50 0.75	Increasing (0.4-0.9)	2	2
SHBPSO-TVAC (R=5)	-	-	-	0	Decreasing (2.5-0.5)	Increasing (0.5-2.5)

Table 6.3: Optimal number and size of PV placement solutions

Method									
CBPSO		BPSO-TVIW		BPSO-TVAC		BPSO-SIIW (n=0.50)		SHBPSO-TVAC	
Bus	Size (MW)	Bus	Size (MW)	Bus	Size (MW)	Bus	Size (MW)	Bus	Size (MW)
4	0.3182	4	0.5197	3	1.4597	2	0.1179	2	2.2958
10	2.1263	5	0.1564	6	0.8787	5	0.5840	7	0.3165
11	0.7444	8	1.4769	9	0.2148	8	0.7845	9	0.4025
14	0.2089	9	0.6160	10	1.1105	10	0.2286	12	0.2860
17	0.3030	11	0.4290	11	0.3706	12	1.8487	13	2.4800
20	0.2259	15	0.5041	13	0.4065	18	0.9522	14	0.3472
25	1.6146	24	0.4163	20	0.2667	19	0.9423	18	0.1096
27	2.5133	27	1.4057	21	0.6670	21	0.3195	20	0.7609
34	1.7022	28	0.0815	23	0.4402	22	0.1243	24	0.3455
36	0.3475	29	0.2931	24	0.2477	24	0.3770	26	0.3106
38	2.1137	30	0.7336	26	0.4877	28	1.0982	30	0.3526
39	0.2195	33	0.6072	29	0.6569	29	0.0974	31	0.4734
40	0.1260	34	0.2124	31	1.8167	36	0.0675	32	0.0583
42	0.2717	35	0.5290	37	0.3860	37	0.7473	35	0.1255
46	0.1215	40	0.2008	38	0.4703	40	0.4745	36	0.8451
47	3.2133	41	1.1120	41	1.0669	42	0.3536	42	0.1252
48	0.4075	43	1.2007	44	0.9033	44	0.1409	43	0.1264
49	0.3244	46	0.0669	50	0.4321	45	0.4111	45	0.3072
50	1.4289	47	1.5938	56	0.7503	48	0.3980	46	0.5009
55	1.7493	55	0.2104			49	0.4932	53	0.9447
57	0.1794	58	1.4061			51	0.3170	56	0.9585
58	0.1465					52	0.1266	57	0.4988
						58	0.2252		
						59	0.5521		

Table 6.4: Objective solutions for minimizing total real power loss

Method	Total PV units (unit)	Total PV size (MW)	Ploss (kW)	Qloss (kVAR)	% Loss reduction	
					Real	Reactive
Original power loss in the 59 bus system			122.2559	278.8729		
CBPSO	22	20.4060	77.3498	174.2723	36.73	37.51
BPSO-TVIW	21	13.7716	32.4893	70.2386	73.43	74.81
BPSO-TVAC	19	13.0326	32.9616	73.4654	73.04	73.66
BPSO-SIIW						
(n=0.25)	32	17.4745	37.3217	78.6389	69.47	71.80
(n=0.50)	24	11.7816	30.6354	68.9230	74.94	75.29
(n=0.75)	27	13.7539	33.1288	74.2084	72.90	73.39
SHBPSO-TVAC	***22***	***12.9712***	***29.4176***	***66.3648***	***75.94***	***76.20***

In Fig. 6.5, the convergence characteristics of five different methods in the 59 bus distribution system are shown. SHBPSO-TVAC with particle movement converges much faster to a better solution than the other four methods on the 59 bus distribution system.

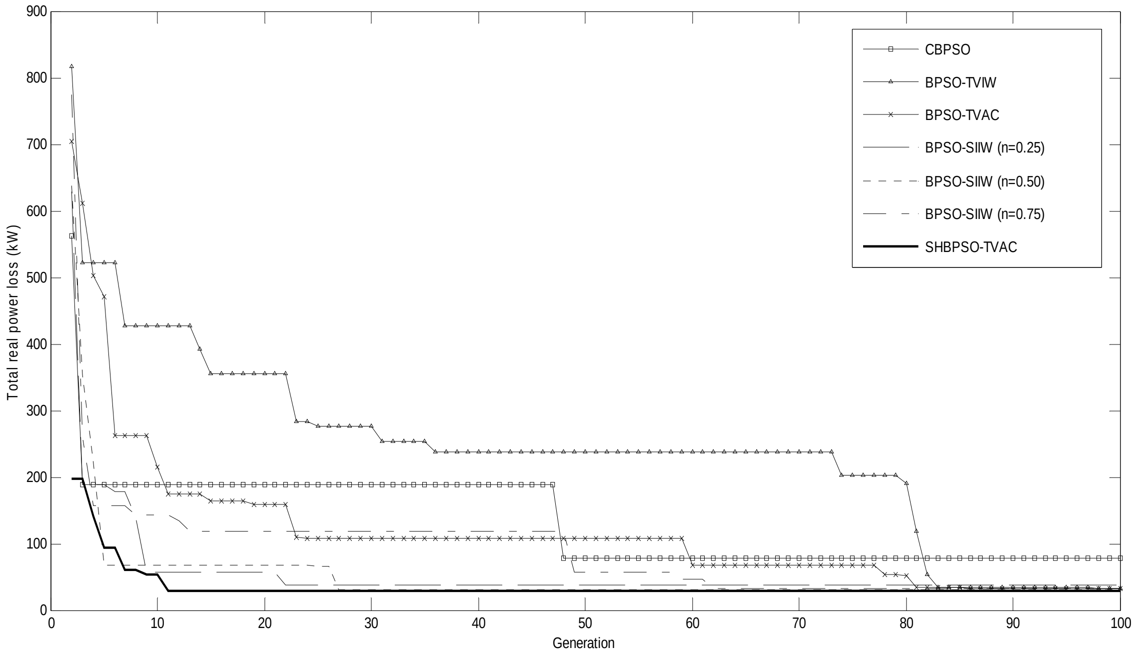

Figure 6.5: Convergence characteristics of the total real power loss

Table 6.5 shows that the average and minimum real power losses of SHBPSO-TVAC are less than the other methods on the 59-bus distribution system with significant smaller standard deviation.

Table 6.5: Statistic variances of PSO types for optimal PV placement

Method	$Ploss_{max}$ (kW)	$Ploss_{avg}$ (kW)	$Ploss_{min}$ (kW)	Standard deviation
CBPSO	252.5132	154.1605	77.3498	56.7742
BPSO-TVIW	164.8912	83.7849	32.4893	43.4613
BPSO-TVAC	136.5418	86.5069	32.9616	38.0505
BPSO-SIIW				
(n=0.25)	73.2308	55.9680	37.3217	13.1928
(n=0.50)	85.2219	46.3915	30.6354	20.0578
(n=0.75)	43.1392	37.3563	33.1288	4.3612
SHBPSO-TVAC	***30.7816***	***29.8797***	***29.4176***	***0.4367***

In order to have a clear comparison, bus voltages in the base case and also after installation of PV units are illustrated in Fig. 6.6. The outcomes represent that installation of PV units considerably improves the voltage profile. Note that installation of PV units give better average voltage levels (0.9710 per unit) compared with the original system (0.9636 per unit). In the system without PV units, the lowest voltage level is 0.9553 per unit. After the PV units are installed, the voltage level are improved (0.9664 – 0.98 per unit) which are within the operating range of $\pm 10\%$.

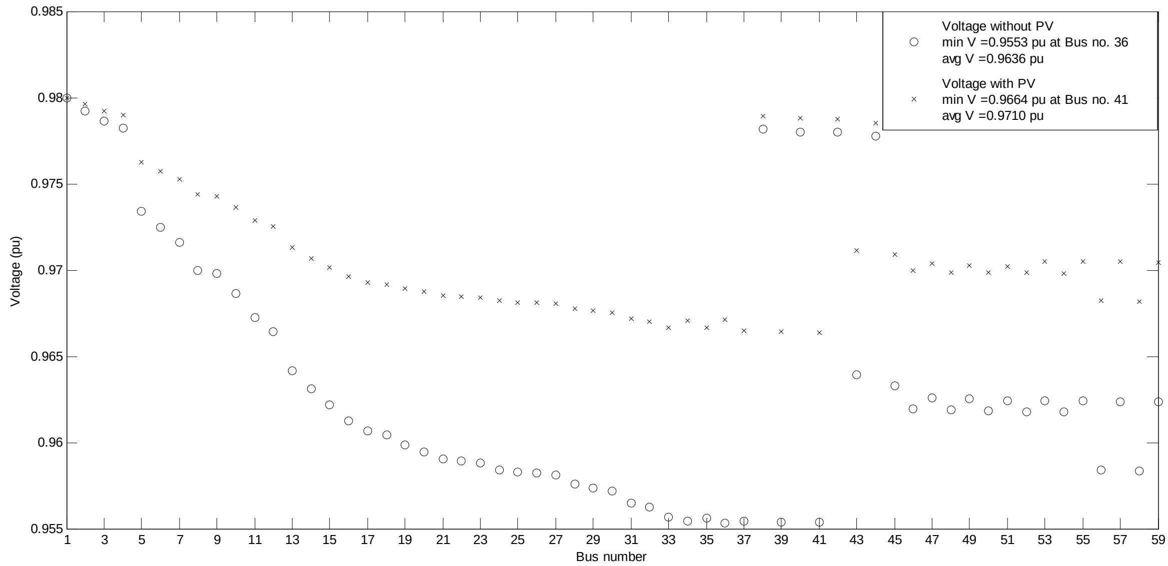

Figure 6.6: Voltage level

Table 6.6 shows the PV power output on a day associated with solar irradiance. The table presents the results of an optimization technique to economic load dispatch problems with considering the hourly solar irradiance.

Table 6.6: Average PV power output (MW) on a day associated with solar irradiance

Month	a.m.						noon	p.m.				
	6.00-7.00	7.00-8.00	8.00-9.00	9.00-10.00	10.00-11.00	11.00-12.00	12.00-1.00	1.00-2.00	2.00-3.00	3.00-4.00	4.00-5.00	5.00-6.00
January	0.033	2.331	***12.971***	***12.971***	***12.971***	***12.971***	***12.971***	***12.971***	***12.971***	***12.971***	***12.971***	9.469
February	0.623	12.122	***12.971***	***12.971***	***12.971***	***12.971***	***12.971***	***12.971***	***12.971***	***12.971***	***12.971***	7.355
March	3.303	12.030	***12.971***	***12.971***	***12.971***	***12.971***	***12.971***	***12.971***	***12.971***	***12.971***	***12.971***	10.601
April	1.912	***12.971***	***12.971***	***12.971***	***12.971***	***12.971***	***12.971***	***12.971***	***12.971***	***12.971***	***12.971***	7.894
May	3.724	8.365	***12.971***	***12.971***	***12.971***	***12.971***	***12.971***	***12.971***	***12.971***	***12.971***	***12.971***	7.796
June	4.016	***12.971***	***12.971***	***12.971***	***12.971***	***12.971***	***12.971***	***12.971***	***12.971***	***12.971***	1.785	1.191
July	2.481	8.547	***12.971***	***12.971***	***12.971***	***12.971***	***12.971***	***12.971***	***12.971***	***12.971***	***12.971***	7.726
August	1.678	5.817	***12.971***	***12.971***	***12.971***	***12.971***	***12.971***	***12.971***	***12.971***	***12.971***	***12.971***	9.388
September	1.956	***12.971***	***12.971***	***12.971***	***12.971***	***12.971***	***12.971***	***12.971***	***12.971***	12.904	9.960	3.826
October	2.063	12.176	***12.971***	***12.971***	***12.971***	***12.971***	***12.971***	***12.971***	***12.971***	***12.971***	***12.971***	6.870
November	3.029	***12.971***	***12.971***	***12.971***	***12.971***	***12.971***	***12.971***	***12.971***	***12.971***	***12.971***	***12.971***	4.297
December	0.319	8.521	***12.971***	***12.971***	***12.971***	***12.971***	***12.971***	***12.971***	***12.971***	***12.971***	***12.971***	10.792

Table 6.7 shows average real and reactive power loss on a day associated with solar irradiance. The maximum loss reduction occurs when the system supplied maximum PV power output. For the solution of load flow problem at transmission level, DG plant can be modeled as injections of active and reactive power.

Table 6.7: Average real and reactive power loss (kW, kVAR) on a day associated with solar irradiance

Month			a.m.				noon			p.m.		
kW kVAR	6.00- 7.00	7.00- 8.00	8.00- 9.00	9.00- 10.00	10.00- 11.00	11.00- 12.00	12.00- 1.00	1.00- 2.00	2.00- 3.00	3.00- 4.00	4.00- 5.00	5.00- 6.00
January	121.770	91.825	***29.410***	***29.410***	***29.410***	***29.410***	***29.410***	***29.410***	***29.410***	***29.410***	***29.410***	36.332
	277.760	209.330	***66.360***	***66.360***	***66.360***	***66.360***	***66.360***	***66.360***	***66.360***	***66.360***	***66.360***	82.340
February	113.510	30.190	***29.410***	***29.410***	***29.410***	***29.410***	***29.410***	***29.410***	***29.410***	***29.410***	***29.410***	46.847
	258.900	68.167	***66.360***	***66.360***	***66.360***	***66.360***	***66.360***	***66.360***	***66.360***	***66.360***	***66.360***	106.440
March	80.929	30.271	***29.410***	***29.410***	***29.410***	***29.410***	***29.410***	***29.410***	***29.410***	***29.410***	***29.410***	32.755
	184.420	68.359	***66.360***	***66.360***	***66.360***	***66.360***	***66.360***	***66.360***	***66.360***	***66.360***	***66.360***	74.113
April	96.845	***29.410***	***29.410***	***29.410***	***29.410***	***29.410***	***29.410***	***29.410***	***29.410***	***29.410***	***29.410***	43.692
	220.800	***66.360***	***66.360***	***66.360***	***66.360***	***66.360***	***66.360***	***66.360***	***66.360***	***66.360***	***66.360***	99.221
May	76.531	41.203	***29.410***	***29.410***	***29.410***	***29.410***	***29.410***	***29.410***	***29.410***	***29.410***	***29.410***	44.242
	174.360	93.516	***66.360***	***66.360***	***66.360***	***66.360***	***66.360***	***66.360***	***66.360***	***66.360***	***66.360***	100.480
June	73.602	***29.410***	***29.410***	***29.410***	***29.410***	***29.410***	***29.410***	***29.410***	***29.410***	***29.410***	98.405	105.940
	167.67	***66.360***	***66.360***	***66.360***	***66.360***	***66.360***	***66.360***	***66.360***	***66.360***	***66.360***	224.370	241.590
July	90.063	40.309	***29.410***	***29.410***	***29.410***	***29.410***	***29.410***	***29.410***	***29.410***	***29.410***	***29.410***	44.622
	205.300	91.465	***66.360***	***66.360***	***66.360***	***66.360***	***66.360***	***66.360***	***66.360***	***66.360***	***66.360***	101.35
August	99.728	57.626	***29.410***	***29.410***	***29.410***	***29.410***	***29.410***	***29.410***	***29.410***	***29.410***	***29.410***	36.646
	227.390	131.120	***66.360***	***66.360***	***66.360***	***66.360***	***66.360***	***66.360***	***66.360***	***66.360***	***66.360***	83.059
September	96.302	***29.410***	***29.410***	***29.410***	***29.410***	***29.410***	***29.410***	***29.410***	***29.410***	29.875	34.607	75.497
	219.560	***66.360***	***66.360***	***66.360***	***66.360***	***66.360***	***66.360***	***66.360***	***66.360***	67.401	78.374	172.000
October	95.012	30.145	***29.410***	***29.410***	***29.410***	***29.410***	***29.410***	***29.410***	***29.410***	***29.410***	***29.410***	49.965
	216.610	68.063	***66.360***	***66.360***	***66.360***	***66.360***	***66.360***	***66.360***	***66.360***	***66.360***	***66.360***	113.580
November	83.887	***29.410***	***29.410***	***29.410***	***29.410***	***29.410***	***29.410***	***29.410***	***29.410***	***29.410***	***29.410***	70.874
	191.180	***66.360***	***66.360***	***66.360***	***66.360***	***66.360***	***66.360***	***66.360***	***66.360***	***66.360***	***66.360***	161.430
December	117.720	40.430	***29.410***	***29.410***	***29.410***	***29.410***	***29.410***	***29.410***	***29.410***	***29.410***	***29.410***	74.429
	268.500	91.743	***66.360***	***66.360***	***66.360***	***66.360***	***66.360***	***66.360***	***66.360***	***66.360***	***66.360***	169.560

Table 6.8 summarized the average power output as well as reduction and residual losses during daytime.

Table 6.8: Summary of monthly averaged energy production

Month	PV output (MWh)	Reduction loss		Residual loss	
		Ploss (MWh)	Qloss (MWh)	Ploss (MWh)	Qloss (MWh)
January	3,985.7940	29.5260	67.5739	15.9532	36.1671
February	3,831.5424	28.3314	64.8398	12.7466	28.8615
March	4,422.8940	32.8111	75.0927	12.6681	28.6483
April	4,185.5760	30.9730	70.8852	13.0391	29.5088
May	4,235.4432	32.2525	73.8072	13.2267	29.9338
June	3,712.0320	27.7329	63.4677	16.2792	36.9263
July	4,200.4752	31.8490	72.8847	13.6302	30.8563
August	4,142.3688	31.2598	71.5375	14.2194	32.2035
September	3,972.4920	29.8652	68.3472	14.1469	32.0468
October	4,273.3500	31.8450	72.8802	13.6342	30.8608
November	4,111.1640	30.5462	69.9074	13.4659	30.4866
December	4,014.9588	30.0638	68.8023	15.4154	34.9387
Summation:	*49,088.0904*	*367.0559*	*840.0258*	*168.4249*	*381.4385*

6.5 Conclusion

In this study, the proposed SHBPSO-TVAC method effectively determines the optimal number and size of PV placement in a PEA distribution system. The reinitialized the particle velocity with time varying acceleration coefficients indicates better search direction than CBPSO, BPSO-TVIW, BPSO-TVAC and BPSO-SIIW. Experimental results indicate that SHBPSO-TVAC can give much faster convergence than other methods on the 59-bus system. Moreover, the optimal PV placement by SHBPSO-TVAC can lead to good PEA policy to manage PV-VSPP allocation for power loss reduction and green energy support.

Chapter 7

Conclusions and Recommendations

The results of the research on application of particle swarm technique for power systems have been summarized to conclude the study. In addition, several recommendations for further research that could be useful when implementing similar projects in future have been made.

7.1 Conclusions

In this study, a methodology of finding the optimal locations and sizes of DG for maximum loss reduction of radial distribution systems is presented.

The PSO algorithm is fast and accurate in determining the sizes and locations. A look up table can be created with using power flow calculation, and can be used to recommend the optimal size of DG at different buses. Different types of DG lead to different sizes and locations to achieve the minimum power loss.

The methodology is tested on a 26 and a 59 bus systems. By installing DG at all potential locations, the total power loss of the system has been reduced drastically and the voltage profile of the system is also improved.

7.2 Recommendations for Further Study

The following recommendations for further research are suggested based on the work carried out in this study.

- The model considered only the PV-VSPP for distributed generation systems. Depending on the locations and available renewable resources, the model can be expanded to include wind and micro-hydropower systems.
- Better results on the system design can be achieved if the electricity demand estimation can include a detailed electricity consumption including the future load for obtaining a clear picture on electricity consumption patterns.
- This approach can further be expanded to conduct the optimal placement for different type of DG.
- The model can include factors for assessing the potential of reducing CO_2 for locations under consideration if a PV-VSPP is implemented.

Author's Publications

Journals

- Phuangpornpitak N, Tia S. Feasibility Study of Wind Farms under the Thai Very Small Scale Renewable Energy Power Producer (VSPP) Program. Energy Procedia 2011;9:159-170.

- Phuangpornpitak N, Tia S., Prommee W. Optimal Photovoltaic Placement by Self-Organizing Hierarchical Binary Particle Swarm Optimization with Solar Irradiance Capability in Thailand, submitted to an International Journal of Renewable and Sustainable Energy Reviews, 2012.

Conferences

- Phuangpornpitak N, Tia S, Prommee W, Phuangpornpitak W. A Study of Particle Swarm Technique for Renewable Energy Power Systems. PEA-AIT International Conference on Energy and Sustainable Development: Issues and Strategies (ESD 2010). Chiang Mai, Thailand, 2010.

- Phuangpornpitak N, Tia S. Assessment of Wind Energy Potential for Electricity Generation in Nakhonphanom Province, Thailand. 9th Eco-Energy and Materials Science and Engineering Symposium. Chiang Rai, Thailand, 2011.

Reference

[1] IEA. World Energy Outlook 2010: International Energy Agency, Paris, France, 2010.

[2] BCSE. Increasing Energy Access in Developing Countries: The Role of Distributed Generation. The Business Council for Sustainable Energy, 2004.

[3] Srisastra P, Limmeechokchai B, Shrestha RM, Shrestha R. Impacts of Distributed Power Generation on Electricity Generation Expansion Planning and CO2 Emission: A Case Study of Thailand. Thammasat International Journal of Science and Technology 2003;8 (2):33-44.

[4] Ackermann T, Andersson G, Söder L. Distributed generation: a definition. Electric Power Systems Research 2001;57 (3):195-204.

[5] Punjad P, Tantimaporn T, Chaiyabin J. Experience of Introducing New Regulatory Policy on Electricity Supply Industry of Thailand. 20th International Conference on Electricity Distribution. Prague, Czech Republic, 2009.

[6] Sritakaew P, Sangswang A, Kirtikara K. On the Reliability Improvement of Distributed Generation Systems Using PV Grid-Connected Systems. ECTI Transactions on Electrical Engineering, Electronics, and Communications 2007;5 (1):79-84.

[7] Medina A, Hernandez JC, Jurado F. Optimal Placement and Sizing Procedure for PV Systems on Radial Distribution Systems. International Conference on Power System Technology. Chongqing, China, 2006.

[8] AlRashidi MR, El-Hawary ME. A Survey of Particle Swarm Optimization Applications in Electric Power Systems. IEEE Transactions on Evolutionary Computation 2009;13 (4):913-8.

[9] Phuangpornpitak N, S. Tia, W. Prommee, and W. Phuangpornpitak. A Study of Particle Swarm Technique for Renewable Energy Power Systems. PEA-AIT International Conference on Energy and Sustainable Development: Issues and Strategies (ESD 2010). Chiang Mai, Thailand, 2010.

[10] Naresh A, Pukar M, Mithulanathan N. An analytical approach for DG allocation in primary distribution network. Electric Power and Energy Systems 2006;28:669-78.

[11] Kumar S, Barua DC, Dung TQ. PV System components: Technology Fact Sheets. Asian Institute of Technology, 2005.

[12] Kumar S, Barua DC, Dung TQ. Technology Packages: Low-cost PV system components. Asian Institute of Technology, 2005.

[13] K Hossain A, Badr O. Prospects of renewable energy utilisation for electricity generation in Bangladesh. Renewable and Sustainable Energy Reviews 2007;11 (8):1617-49.

[14] Lidula NWA, Mithulananthan, N., Ongsakul, W., Widjaya, C. and Henson, R. ASEAN towards clean and sustainable energy: Potentials, utilization and barriers. Renewable Energy 2007;32 (9):1441-52.

[15] Urmee T, Harries D, Schlapfer A. Issues related to rural electrification using renewable energy in developing countries of Asia and Pacific. Renewable Energy 2009;34 (2):354-7.

[16] Kennedy J, Eberhart R. Particle Swarm Optimization. In: IEEE Proceedings of the International Conference on Neural Networks. Perth, Australia, 1995. pp. 1942-8.

[17] Prommee W, Ongsakul W. Optimal Multi-Distributed Generation Placement by Adaptive Weight Particle Swarm Optimization. International Conference on Control, Automation and Systems. Seoul, Korea, 2008. pp. 1663-8.

[18] Krueasuk W. Optimal placement of distributed generation using particle swarm optimization. Energy Field of Study: Asian Institute of Technology, Thailand, 2006. pp. 35.

[19] El-Fouly THM, Zeineldin, H. H., El-Saadany, E. F. and Salama, M. M. A. A new optimization model for distribution substation siting, sizing, and timing. International Journal of Electrical Power & Energy Systems 2008;30 (5):308-15.

[20] Hakimi SM, Moghaddas-Tafreshi SM. Optimal sizing of a stand-alone hybrid power system via particle swarm optimization for Kahnouj area in south-east of Iran. Renewable Energy 2009;34 (7):1855-62.

[21] Kornelakis A, Marinakis Y. Contribution for optimal sizing of grid-connected PV-systems using PSO. Renewable Energy 2009;35 (6):1333-41.

[22] Gómez M, López A, Jurado F. Optimal placement and sizing from standpoint of the investor of Photovoltaics Grid-Connected Systems using Binary Particle Swarm Optimization. Applied Energy 2010;In Press, Corrected Proof.

[23] Kashefi Kaviani A, Riahy GH, Kouhsari SM. Optimal design of a reliable hydrogen-based stand-alone wind/PV generating system, considering component outages. Renewable Energy 2009;34 (11):2380-90.

[24] Lingfeng W, Singh C. Compromise Between Cost and Reliability In Optimum Design of An Autonomous Hybrid Power System Using Mixed-Integer PSO Algorithm. International Conference on Clean Electrical Power (ICCEP 07), 2007. pp. 682-9.

[25] Lingfeng W, Singh C. PSO-Based Multi-Criteria Opyimum Design of A Grid-Connected Hybrid Power System With Multiple Renewable Sources of Energy. Proceedings of the 2007 IEEE Swarm Intelligence Symposium (SIS 2007). Hanolulu, Hawaii, USA, 2007.

[26] Siahkali H, Vakilian M. Electricity generation scheduling with large-scale wind farms using particle swarm optimization. Electric Power Systems Research 2009;79 (5):826-36.

[27] Ünler A. Improvement of energy demand forecasts using swarm intelligence: The case of Turkey with projections to 2025. Energy Policy 2008;36 (6):1937-44.

[28] El-Telbany M, El-Karmi F. Short-term forecasting of Jordanian electricity demand using particle swarm optimization. Electric Power Systems Research 2008;78 (3):425-33.

[29] Sedighizadeh M, Fallahnejad M, Alemi MR, Omidvaran M, Arzaghi-haris D. Optimal Placement of Distributed Generation Using Combination of PSO and Clonal Algorithm. 2010 IEEE International Conference on Power and Energy (PECon2010). Kuala Lumpur, Malaysia, 2010.

[30] Krueasuk W. Particle Swarm Optimization for Optimal DG Placement in Distribution System. The 2007 ECTI International Conference. Chiang Rai, Thailand, 2007.

[31] El-Khattam W, Bhattacharya K, Hegazy Y, Salama MMA. Optimal investment planning for distributed generation in a competitive electricity market. IEEE Transaction on Power Systems 2004;19:1674-84.

[32] Yu X, Xiong X, Wu Y. A PSO-based approach to optimal capacitor placement with harmonic distortion consideration. Electric Power Systems Research 2004;71:27-33.

[33] El-Zonkoly AM. Optimal placement of multi-distributed generation units including different load models using particle swarm optimization. Swarm and Evolutionary Computation 2011;1 (1):50-9.

[34] Phuangpornpitak N, Tia S. Assessment of Wind Energy Potential for Electricity Generation in Nakhonphanom Province, Thailand. 9th Eco-Energy and Materials Science and Engineering Symposium. Chiang Rai, Thailand, 2011.

[35] Phuangpornpitak N, Tia S. Feasibility Study of Wind Farms Under the Thai very small Scale Renewable Energy Power Producer (VSPP) Program. Energy Procedia 2011;9:159-70.

[36] Shi Y, Eberhart RC. A modified particle swarm optimizer. Proceedings of IEEE International Conference on Evolutionary Computation 1998:69-73.

[37] Shi Y, Eberhart RC. Empirical study of particle swarm optimization. Proceedings of IEEE International Conference on Evolutionary Computation 1999:101-6.

[38] Prommee W, Ongsakul W. Opimal multiple distributed generation placement in microgrid system by improved reinitialized social structures particle swarm optimization. European Transactions on Electrical Power 2010.

[39] Suganthan PN. Particle swarm optimizer with neighborhood operator. Proceedings of IEEE International Conference on Evolutionary Computation 1999:1958-62.

[40] Boonchuay C, Ongsakul W. Optimal risky bidding strategy for a generating company by self-organising hierarchical particle swarm optimisation. Energy Conversion and Management 2011;52 (2):1047-53.

[41] Ratnaweera A, Halgamuge SK, Watson HC. Self-organizing hierarchical particle swarm optimizer with time-varying acceleration coefficients. IEEE Transaction on Evolutionary Computation 2004;8 (3):240-55.

[42] Chaturvedi KT, Pandit M, Srivastava L. Self-organizing hierarchical particle swarm optimization for nonconvex economic dispatch. IEEE Transaction on Power Systems 2008;23 (3):1079-87.

[43] Thongpull B. Optimal Siting and Sizing of Distributed Generator for Loss Reduction Considering Fault Level in Distribution Network Systems. Department of Electrical Engineering: Kasetsart University, Thailand, 2009. pp. 125.

[44] Hedayati H, Nabaviniaki S. A new method for placement of DG unit in distribution networks. IEEE Power System Conference and Exposition. Atlanta, Georgia, USA, 2006.

[45] Shukla TN, Singh SP, Naik KB. Allocation of optimal distributed generation using GA for minimum system losses in radial distribution networks. International Journal of Engineering, Science and Technology 2010;2 (3):94-106.

[46] Popovic DH, J.A. Greatbanks, M. Begovic, and A. Pregelj. Placement of distributed generators and reclosers for distribution network security and reliability. International Journal of Electrical Power and Energy System 2005;27:398-408.

[47] Prommee W, Ongsakul W. Optimal multiple distributed generation placement in microgrid system by improved reinitialized social structures particle swarm optimization. European Transactions on Electrical Power 2011;21:489-504.

[48] Yang J, J. Zhou, L. Liu, and Y. Li. A novel strategy of pareto-optimal solution searching in multi-objective particle swarm optimization (MOPSO). Computers & Mathematics with Applications 2009;57 (11-12):1995-2000.

[49] Sahoo NC, Ganguly S, Das D. Simple heuristics-based selection of guides for multi-objective PSO with an application to electrical distribution system planning. Engineering Applications of Artificial Intelligence 2011;24 (4):567-85.

[50] Cai J, X. Ma, Q. Li, L. Li, and H. Peng. A multi-objective chaotic particle swarm optimization for environmental/economic dispatch. Energy Conversion and Management 2009;50 (5):1318-25.

[51] Yuan X, H. Nie, A. Su, L. Wang, and Y. Yuan. An improved binary particle swarm optimization for unit commitment problem. Expert Systems with Applications 2009;36 (4):8049-55.

[52] Rahman MH, Yamashiro S. Novel Distributed Power Generating System of PV-ECaSS Using Solar Energy Estimation. IEEE Transactions on Energy Conversion 2007;22 (2):358-67.

[53] Eltawil MA, Zhao Z. Grid-connected photovoltaic power systems: Technical and potential problems--A review. Renewable and Sustainable Energy Reviews 2011;14 (1):112-29.

[54] Chupong C, Plangklang B. Forecasting power output of PV grid connected system in Thailand without using solar radiation measurement. Energy Procedia 2011;9:230-7.

[55] Chirarattananon S, Chaiwiwatworakul P. Distributions of sky luminance and radiance of North Bangkok under standard distributions. Renewable Energy 2007;32 (8):1328-45.

[56] Notton G, Lazarov V, Stoyanov L. Optimal sizing of a grid-connected PV system for various PV module technologies and inclinations, inverter efficiency characteristics and locations. Renewable Energy 2010;35:541-54.

[57] Gómez M, López A, Jurado F. Optimal placement and sizing from standpoint of the investor of Photovoltaics Grid-Connected Systems using Binary Particle Swarm Optimization. Applied Energy 2010;87 (6):1911-8.

[58] Boonchuay C, W. Ongsakul, J. Zhong, and F.F. Wu. Optimal trading strategy for GenCo in LMP-based and bilateral markets using self-organising hierarchical PSO. International Journal of Engineering, Science and Technology 2010;2 (3):82-93.

[59] Phuangpornpitak N, Tia S, Prommee W. Optimal Photovoltaic Placement by Self-Organizing Hierarchical Binary Particle Swarm Optimization with Solar Irradiance Capability in Thailand. Submitted to an International Journal of Renewable and Sustainable Energy Reviews 2012.